ORIGINAL ARTICLE
Iran J Allergy Asthma Immunol.
December 2024; 23(6):699-726.
DOI: 10.18502/ijaai.v23i6.17380

A Novel Prognostic Immune-related Gene Signature in Hepatocellular Carcinoma Through Bioinformatics and Experimental Approaches

Atieh Pourbagheri-Sigaroodi[1], Majid Momeny[2], Nima Rezaei[3,4,5], Fatemeh Fallah[1], and Davood Bashash[6]

[1] Pediatric Infections Research Center, Research Institute for Children's Health, Shahid Beheshti University of Medical Sciences, Tehran, Iran
[2] Hematology, Oncology and Stem Cell Transplantation Research Center, Tehran University of Medical Sciences, Tehran, Iran
[3] Research Center for Immunodeficiencies, Children's Medical Center Hospital, Tehran University of Medical Sciences, Tehran, Iran
[4] Network of Immunity in Infection, Malignancy and Autoimmunity (NIIMA), Universal Scientific Education and Research Network (USERN), Tehran, Iran
[5] Department of Immunology, School of Medicine, Tehran University of Medical Sciences, Tehran, Iran
[6] Department of Hematology and Blood Banking, School of Allied Medical Sciences, Shahid Beheshti University of Medical Sciences, Tehran, Iran

Received: 22 April 2024; Received in revised form: 22 June 2024; Accepted: 24 June 2024

ABSTRACT

Despite therapeutic advancements, treatment failure in hepatocellular carcinoma (HCC) continues to pose a significant obstacle. Given the vital role of the tumor immune microenvironment (TIM) in HCC and the promising effectiveness of immune therapies, we aimed to elucidate potential predictive biomarkers by developing a prognostic model based on immune-related genes (IRGs).

After obtaining data, differentially expressed IRGs were identified, and prognostic models were developed using Cox regression analyses. Key contributors of the model were identified and the results were validated by experimental assays in HCC cell lines.

Our eight-IRG signature can serve as an independent prognostic factor in HCC. The low-risk group exhibited superior overall survival and lower tumor mutation burden (TMB). The high-risk group showed elevated proportions of immune cells, including regulatory T cells and resting $CD4^+$ memory T cells. We found that the NEAT1-C1/miR-542-5p/BIRC5 regulatory network may serve as a potential target in HCC. The experimental investigations showed that BIRC5 inhibition reduced the metabolic activity in four HCC cell lines.

The results of this study facilitate patient stratification and the development of more effective treatment strategies, particularly for high-risk HCC patients.

Keywords: Bioinformatics; BIRC5; Hepatocellular carcinoma; Immune-related signature; Prognostic model; Survivin

Corresponding Authors: Fatemeh Fallah, PhD;
Pediatric Infections Research Center, Research Institute for Children's Health, Shahid Beheshti University of Medical Sciences, Tehran, Iran. Tel: (+98 21) 2222 6941, Fax: (+98 21) 2222 6941, Email: dr_fallah@yahoo.com

Davood Bashash, PhD;
Department of Hematology and Blood Banking, School of Allied Medical Sciences, Shahid Beheshti University of Medical Sciences, Tehran, Iran. Tel: (+98 21) 2271 7504, Fax: (+98 21) 2272 1150, Email: d.bashash@sbmu.ac.ir

INTRODUCTION

Hepatocellular carcinoma (HCC) is the seventh most prevalent cancer and the fourth leading cause of cancer-related fatalities worldwide. It primarily arises from liver cirrhosis, which is often triggered by hepatitis viruses and alcohol consumption.[1,2] Moreover, nonalcoholic fatty liver disease (NAFLD) and its specific stage, nonalcoholic steatohepatitis (NASH), which can result from metabolic syndromes such as obesity and type 2 diabetes[3] have been shown to exhibit the most rapid increase as a cause of HCC in Europe, the United States, and Southeast Asia.[4] HCC has a progressive nature, and without early intervention, it can lead to irreversible damage. Despite the advancements in various treatment options such as surgery, chemotherapy, radiotherapy, immunotherapy, and targeted treatments,[5] the prognosis for HCC patients remains discouraging due to high rates of multidrug resistance, metastasis, and recurrence.[6, 7] It is important to note that the Barcelona Clinic Liver Cancer (BCLC) staging system has been widely used over the past few decades to categorize risk groups and predict the prognosis of HCC patients.[1] However, the BCLC primarily focuses on clinical factors and does not account for the molecular heterogeneity of the disease, leading to a growing interest in exploring the prognostic values of molecular features.

The initial proposal of the hallmarks of cancer referred to a set of functional capabilities that human cells gain as they progress from a normal state to a cancerous state.[8] With the discovery of numerous genetic factors associated with cancer development, it has become increasingly evident that immune-related genes (IRGs) play a more significant role than initially thought.[9] Extensive research has demonstrated that IRGs, responsible for regulating the immune responses, play a crucial role in various types of human malignancies,[10-12] including HCC.

Previous research has demonstrated that the dysregulation of IRGs can have a significant impact on the tumor microenvironment, leading to immune evasion and tumor progression.[13, 14] It has been reported that IRGs can also affect the efficacy of immunotherapy by influencing the recruitment and activity of tumor-infiltrating lymphocytes (TILs) in HCC. [15] Specifically, the alteration of certain IRGs is associated with an increased infiltration of immune cells, particularly those participating in the expansion of T cells and natural killer (NK) cells; an event, which in turn results in a more favorable reaction to immune checkpoint inhibitors (ICIs).[16, 17] In addition to the aforementioned importance, it is necessary to discuss IRGs in greater depth, as these genes hold promise as prognostic markers and can serve as potential targets for therapies in HCC. Hence, comprehending the function and expression of IRGs is crucial in deciphering the complex association between the immune system and tumor cells in HCC.

To provide a more comprehensive overview, a schematic depiction of the intricate immune microenvironment of HCC, along with its complex pathogenesis, is shown in Figure 1. Taken altogether, this research demonstrates that the novel eight-IRGs prognostic signature, with a focus on BIRC5 (Survivin), holds promise in predicting the survival of this malignancy, which will not only aid in improved stratification but also lay the groundwork for more efficient treatment approaches in high-risk HCC patients.

MATERIALS AND METHODS

Data Collection

To collect the transcription profiles and clinical data of HCC patients, we utilized the R package "TCGAbiolinks" to retrieve the data from the Cancer Genome Atlas (TCGA) portal available at https://portal.gdc.cancer.gov/. The TCGA portal provided us with 50 samples categorized as normal and 374 samples classified as cancerous. The complete list of IRGs was again acquired from the Immunology Database and Analysis Portal (ImmPort) database (https://immport.niaid.nih.gov). The specific list can be found in Supplementary Table 1. Supplementary Table 2 provides details on the clinical features of the HCC samples in the training, testing, and entire cohorts.

Discovery of Differentially Expressed Genes (DEGs)

Upon normalizing the TCGA dataset, we aimed to uncover the essential IRGs that played a pivotal role in the progression of HCC. To accomplish this, we employed the `limma` package[18] to accurately identify genes that exhibited differential expression (DEGs) between the cancerous and normal samples. Our criteria for determining significance were based on genes with

|logFC| values exceeding 2 and adjusted *p*-values less than 0.01. By integrating the IRGs extracted from the ImmPort database, we successfully pinpointed a distinct set of IRGs that showed differential expression (DE-IRGs). These DE-IRGs were selected for further analysis.

Exploring Functional Enrichment

To gain deeper insights into the potential molecular mechanisms of DE-IRGs, we conducted comprehensive analyses to explore functional enrichment. We employed the "clusterProfiler" R package,[19] a robust tool for investigating functional associations, to carry out Gene Ontology (GO) and Kyoto Encyclopedia of Genes and Genomes (KEGG) enrichment assessments. Statistical significance was determined by a *p* values threshold of less than 0.05, enabling the identification of meaningful and biologically relevant enrichments within the GO categories and KEGG pathways associated with the DE-IRGs.

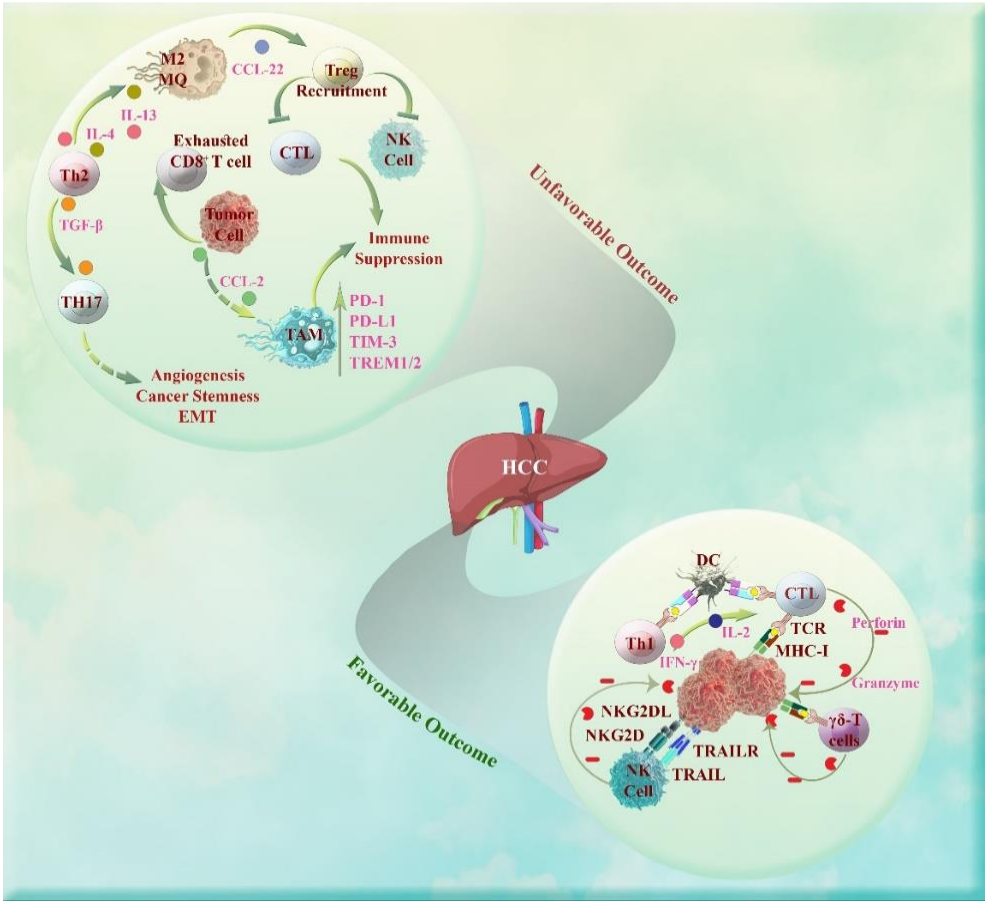

Figure 1. Immune cell interactions in hepatocellular carcinoma (HCC). On one hand, T helper 2 (Th2) cells induce the differentiation of M2 macrophages (MQ), which in turn recruit regulatory T cells (Treg). Treg cells exert an inhibitory effect on cytotoxic T lymphocytes (CTL) and natural killer (NK) cells, impairing their antitumor functions. Th2 cells also activate Th17 cells, leading to processes such as angiogenesis and epithelial-mesenchymal transition (EMT). Furthermore, not only do HCC tumors induce T cell exhaustion but also manipulate the tumor microenvironment (TME) by inducing the differentiation of tumor-associated macrophages (TAM) into a phenotype with high expression of PD-1, PD-L1, TIM-3, and TREM1/2; further contributing to immune suppression and tumor evasion. On the other hand, dendritic cells (DCs) via antigen presentation activate CTL and Th1 cells. IL-2 secreted by Th1 acts as a growth factor for CTL, promoting their proliferation and enhancing their cytotoxic capabilities. IFN-γ also activates CTL and enhances their ability to recognize and kill tumor cells. Gamma delta (γδ) T cells contribute to the immune response against HCC by producing perforin and granzyme, similar to NK cells, which recognize tumor cells through the NKG2D receptor and induce tumor cell death through the release of perforin, granzyme, and TNF-related apoptosis-inducing ligand (TRAIL).

Creation and Verification of a Prognostic Prediction Model Using Risk Score

In this stage, we undertook a specific process to develop a prognostic prediction model based on a risk score. Firstly, we excluded normal samples and those with missing survival data, focusing exclusively on the remaining TCGA-LIHC cohort. To ensure the robustness of our model, we randomly divided the cohort into training and testing sets. The training set served as the foundation for identifying prognostic IRGs and establishing the prognostic risk model, while the testing set was used for validation.

To identify potential DE-IRGs with prognostic value, we performed univariate Cox regression analysis on the screened DE-IRGs using the powerful `survminer` and `survival` R packages. The result of univariate Cox analyses can be found in Supplementary Table 3. This analysis allowed us to identify genes that have significant potential in predicting patient outcomes. To refine the model and address overfitting concerns, we employed the cutting-edge technique of least absolute shrinkage and selection operator (LASSO) penalized Cox proportional hazards regression. This technique was implemented using the `glmnet` R package,[20] enabling us to select the optimal genes for constructing the model.

Subsequently, we calculated the risk score for each HCC patient by combining gene expression levels with the corresponding multivariate Cox regression coefficients. The risk score was determined using the following formula:

Risk score= (expression of first gene × coefficient of first gene) + (expression of second gene × coefficient of second gene) + ... + (expression of last gene × coefficient of last gene).

To validate the model, we utilized 30% of the TCGA-LIHC samples as the internal test set. Additionally, we performed a Kaplan-Meier (KM) curve analysis to further assess and strengthen the predictive capability of the risk signature.

Assessment of the Established Immune-related Gene Signature

To thoroughly evaluate the potential of the established immune-related signature, our initial task was to determine the optimal threshold for risk score classification. This was achieved by utilizing the `surv_cutpoint` function from the `survminer` package, which enabled us to identify the most suitable cut-off value for risk stratification. The prognostic value of the DE-IRG model was assessed using the widely-used KM analysis technique. By leveraging the powerful `survminer` and `survival` R packages, we investigated the survival of patients based on their risk scores.

To further evaluate the sensitivity and specificity of our signature, we performed receiver operating characteristic (ROC) curve analyses. Specifically, we focused on the 1-, 3-, and 5-year time points and calculated the area under the curve (AUC) using the reliable `survivalROC` R package.[21] These analyses provided valuable insights into the discriminatory power of our risk signature.

In order to determine the independent prognostic significance of the risk score, as well as the clinicopathological features such as gender, age, and TNM stage, we executed both univariate and multivariate Cox regression analyses. These analyses enabled us to assess the individual contributions of each factor in predicting patient outcomes. Additionally, to gain a more profound knowledge of the association between the risk signature and various clinicopathological features, we utilized the Wilcoxon test to explore potential differences in clinicopathological characteristics among patients stratified by their risk scores.

Shedding Light on the Role of Tumor-infiltrating Immune Cells (TIICs)

To gain deeper insights into the intricate dynamics between the tumor microenvironment and our immune-related risk signature, we embarked on an investigation focusing on tumor-infiltrating immune cells (TIICs). By leveraging the robust capabilities of the CIBERSORT method, we utilized gene expression profiles to accurately determine the cellular composition of complex tissues. Additionally, employing the CIBERSORT method allowed us to calculate the immune cell infiltration status for each sample, revealing the presence and abundance of various immune cell types within the tumor microenvironment. To explore the connection between risk scores and immune infiltrating cells, we conducted a Spearman correlation analysis. Through this analysis, we aimed to uncover potential associations and elucidate the influence of immune cell infiltration on the risk signature.

Construction of a Nomogram for Predicting Overall Survival (OS)

We utilized the `rms` R package to develop a nomogram that predicts OS in patients with HCC. The nomogram incorporated variables such as age, gender, stage, TNM classification, and the prognostic risk score model. To assess the correctness of the nomogram, time-dependent calibration curves were generated to evaluate its reliability.

Analysis of Mutations

To obtain comprehensive mutation data, we accessed the tumor mutation burden (TMB) and Mutation Annotation Format (MAF) datasets from the TCGA portal using the `maftools` R package.[22] This tool allowed us to analyze and interpret the genetic alterations present in HCC samples. By utilizing various analytical techniques provided by the `maftools` package, we gained valuable insights into the mutational profile of HCC, including the types of mutations, their frequency, and potential driver mutations.

Identification of Key Contributors Based on the Prognostic Model

HCC samples of TCGA were divided into low- and high-expression based on each gene's optimal cutoff which calculate by the time-dependent ROC. To assess the prognostic value of each gene, the KM analysis was performed using `survminer` and `survival` R packages. Moreover, to evaluate their sensitivity and specificity, the ROC curve analysis of 1-, 3-, and 5-year outcomes were conducted. The AUC was computed using the `survivalROC` R package.

Construction of lncRNA-miRNA-mRNA Regulatory Axis

miRTargetLink and miRTarBase were applied to explore the miRNA targets of the BIRC5 gene. To investigate the lncRNA targets of the miRNA, we used miRNet and LncBase. We also analyzed the expression and prognostic values of miRNAs with Student's t-test and univariate Cox regression coefficient on the TCGA LIHC dataset. Relevant links are as follows:

- miRTargetLink: https://ccb-compute.cs.uni-saarland.de/mirtargetlink2
- miRTarBase:https://mirtarbase.cuhk.edu.cn/~miRTarBase/miRTarBase_2022/php/index.php
- miRNet: https://www.mirnet.ca/upload/MirUploadView.xhtml
- LncBase: https://diana.e-ce.uth.gr/lncbasev3/interactions

Cell lines, Reagents, WST-1 assay, and Quantitative Real-time PCR

The Huh7 (Japanese Collection of Research Bioresources Cell Bank (JCRB)), Hep3B2, SNU449, and HePG2 cell lines (The American Type Culture Collection (Manassas, Virginia)) were cultivated in DMEM medium enriched with antibiotics, 10% fetal bovine serum (Invitrogen), and 2 mM l-glutamine (Invitrogen). The cells were grown in a controlled environment with 5% CO_2 at 37°C. To investigate the impact of a potent inhibitor of BIRC5 (YM155) (Adooq Bioscience, Irvine, California), the cells were exposed to increasing concentrations of the inhibitor. As a negative control, an identical volume of DMSO (Sigma-Aldrich, USA) was added to the control samples, ensuring that the final concentration of DMSO did not exceed 0.1% of the total volume.

To assess the inhibitory effects of YM155 on the metabolic activity of HCC cell lines, the HCC cell lines were treated in 96-well plates. The following day, the cells were exposed to ascending concentrations of the inhibitor for up to 48 hours, while untreated cells served as the control group. After removing the liquid medium, the cells were incubated with WST-1 solution (Roche). The resulting formazan crystals were dissolved in DMSO, and the absorbance was measured using an enzyme-linked immunosorbent assay (ELISA) reader (BioTek Synergy HTX Multimode Reader).

To Analyze the basal gene expression of BIRC5, RNA was extracted from untreated HCC cells and quantified using a Nanodrop instrument. After cDNA synthesis quantitative reverse transcription-PCR (qRT-PCR) analysis was done. The target gene expression levels were normalized to GAPDH levels. The sequences of the primers are included in Supplementary Table 4.

Drug Sensitivity Prediction

The Genomics of Drug Sensitivity in Cancer (GDSC) database was used to calculate the sensitivity of the drug YM155, including its half-maximal inhibitory concentration (IC50) for each sample. This was done using the "oncoPredict" software package. Additionally, the Wilcoxon rank-sum test was performed to assess the difference in sensitivity scores between patients classified as high-risk and low-risk.

Statistical Analysis

We performed statistical analyses using R software version 4.2.1 and GraphPad Prism version 9.5. The R package `pheatmap`[23] was employed to visualize the expression patterns of different genes or variables through heatmaps, enabling the identification of patterns, clusters, and trends within datasets. For the visualization of differential gene expression, we utilized the `ggplot2` package in R[24] to generate volcano plots that effectively highlight genes with significant changes in expression between different groups. The magnitude of change was represented on the x-axis and statistical significance on the y-axis. To analyze the overlap between different sets of elements or datasets, we utilized the Venn diagram tool. The flowchart of the study is depicted in Figure 2. In the experimental analysis, data are presented as the mean ± standard deviation obtained from three separate evaluations.

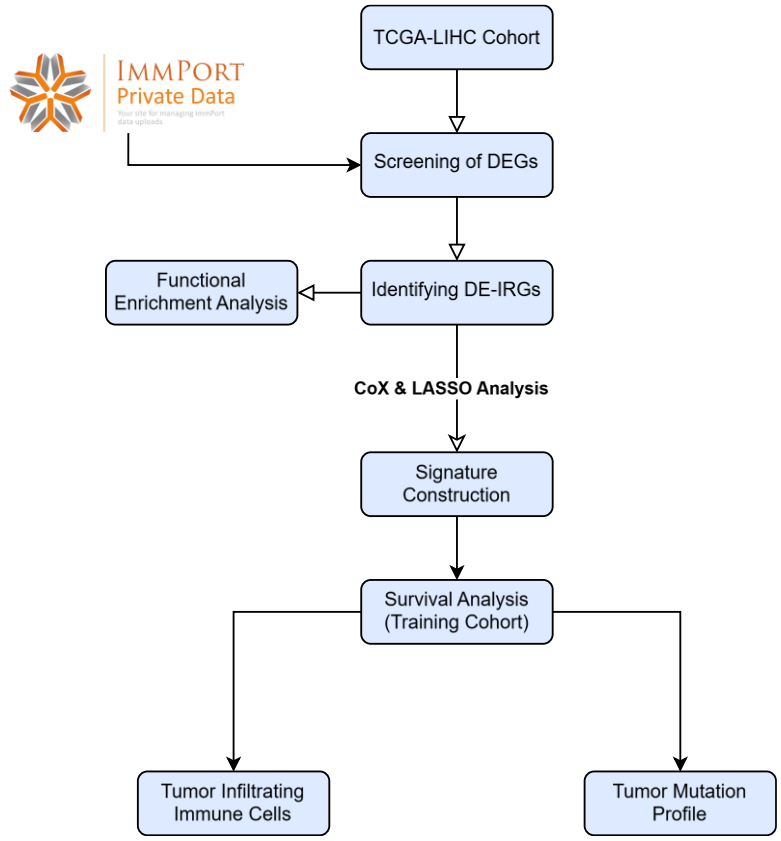

Figure 2. Flowchart illustrating the study's progression. TCGA-LIHC: The Cancer Genome Atlas-Liver Hepatocellular Carcinoma; DEGs: differentially expressed genes; DE-IRGs: differentially expressed immune-related genes; LASSO: least absolute shrinkage and selection operator.

RESULTS

Patient Attributes

In this study, we included RNA-sequencing expression landscape and patients' medical records from 50 normal samples and 374 HCC samples obtained from the TCGA database. These samples were categorized into training (n=257) and testing (n=110) cohorts randomly. Six samples were excluded due to data defects. Supplementary Table 2 provides details on the clinical features of the HCC samples in the training, testing, and entire cohorts, demonstrating no substantial alterations between them (p>0.05).

Identification of Differentially Expressed Immune-related Genes (DE-IRGs)

By applying the criteria of adjusted p value<0.01 and log2 (fold change) more than 2, we identified a total of

428 DEGs between the normal and HCC samples from the TCGA-LIHC project (Figure 3A). After integrating 1796 IRGs, we identified 67 DE-IRGs (Figure 3B). Among these, 6 DE-IRGs were upregulated, while 61 DE-IRGs were downregulated. The expression profiles of the DE-IRGs in normal and cancerous samples are depicted in Figure 3C.

Analysis of Functional Enrichment

To gain better insights into the underlying mechanisms and prognostic implications of HCC, we conducted a functional enrichment analysis to explore the functions and pathways influenced by the 67 DE-IRGs. Gene Ontology (GO) analysis revealed the most meaningful enriched terms for biological process, molecular function, and cellular component, which were "humoral immune response," "immunoglobulin receptor binding," and "blood microparticle," respectively, with an adj. *p*-value less than 0.05. The top eight extremely enriched terms for each of the three ontologies are presented in Figure 4 and Table 1. Additionally, we performed a KEGG pathway analysis using data from the TCGA cohort to recognize possible signaling pathways related to the DE-IRGs (Figure 5, Table 2).

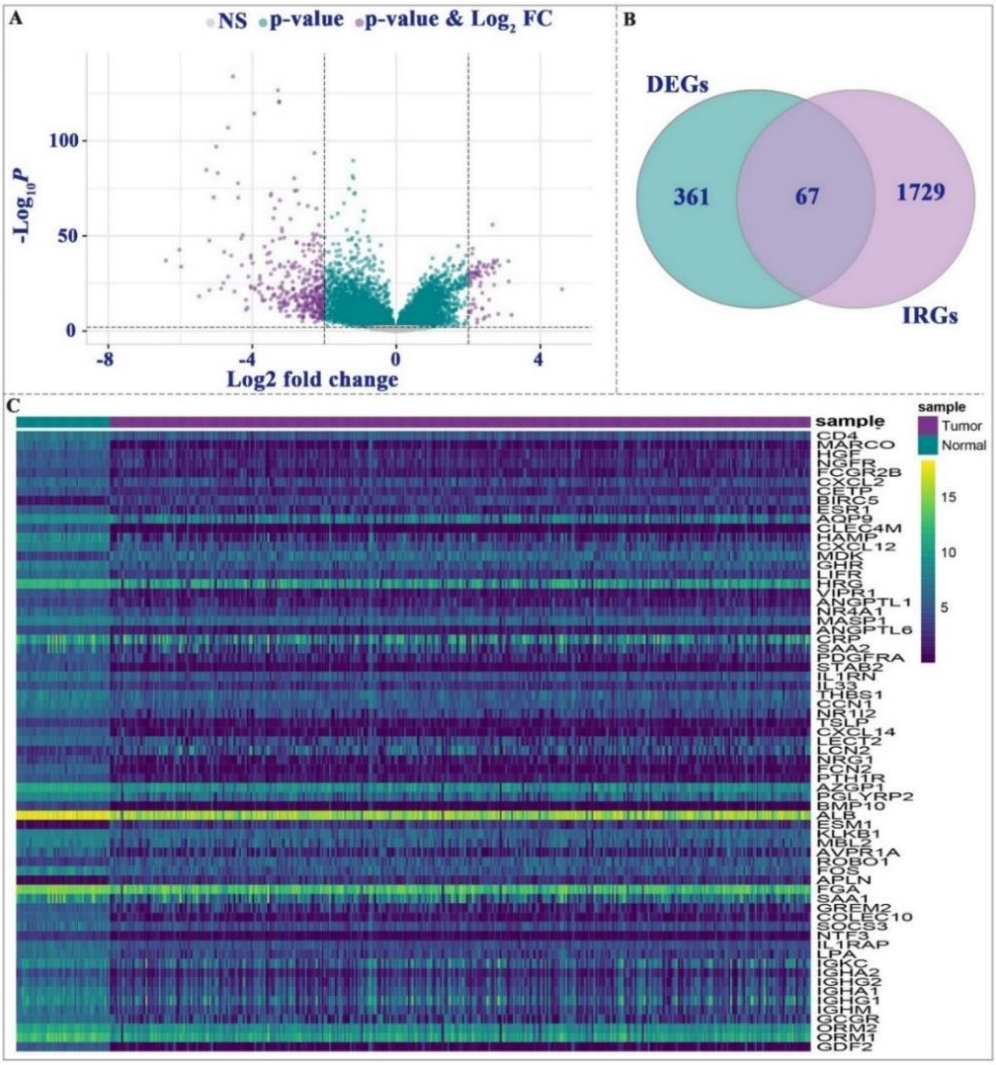

Figure 3. Discovery of differentially expressed immune-related genes (DE-IRGs) between hepatocellular carcinoma (HCC) and non-cancerous samples. A: Volcano plot illustrating differentially expressed genes (DEGs) based on The Cancer Genome Atlas Liver Hepatocellular Carcinoma (TCGA-LIHC) project. B: Venn diagram displaying the overlap between HCC DEGs and IRGs. C: Heatmap showcasing the expression levels of DE-IRGs between normal and tumor samples.

Published by Tehran University of Medical Sciences (http://ijaai.tums.ac.ir)

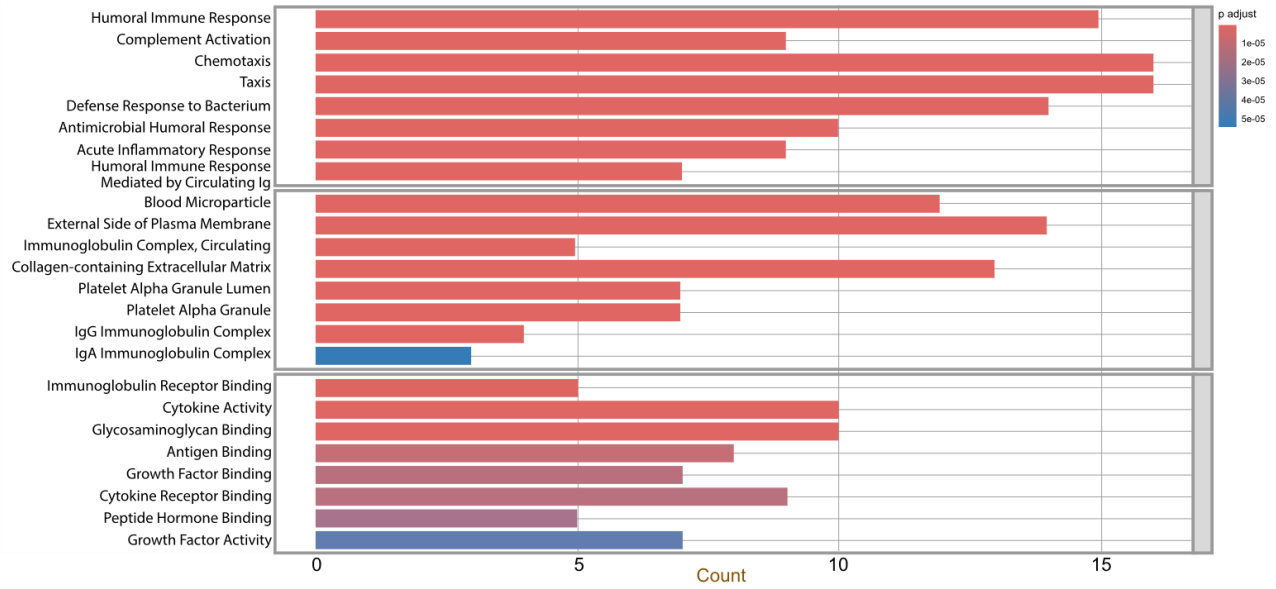

Figure 4. The most significantly enriched Gene Ontology (GO) classes for the confirmed differentially expressed immune-related genes (DE-IRGs). Ig: Immunoglobulin.

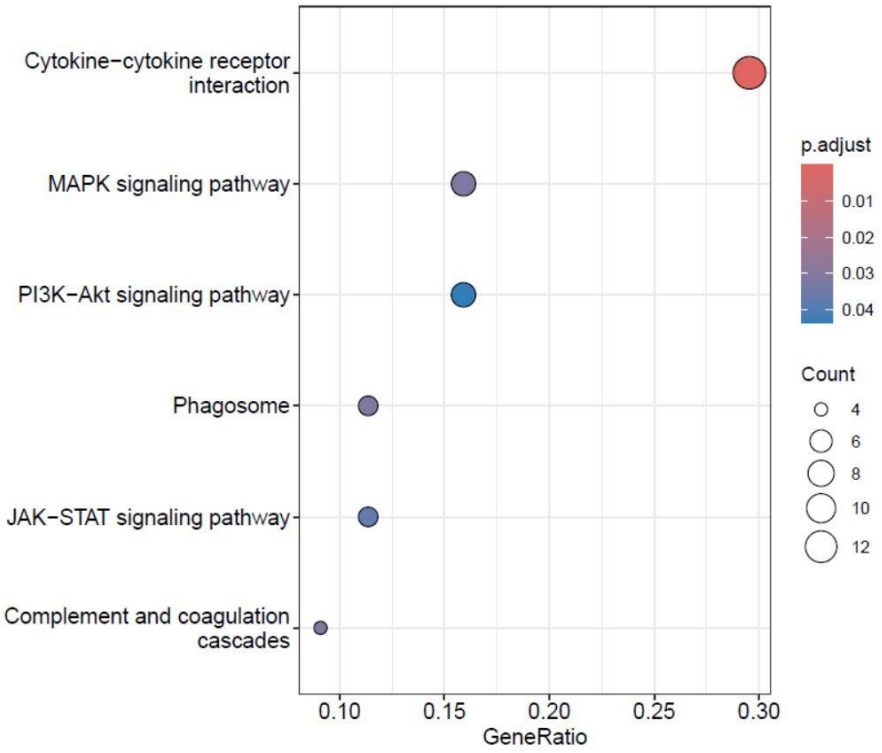

Figure 5. The top 10 most considerably enriched pathways for differentially expressed immune-related genes (DE-IRGs) (adjusted *p*-value < 0.05). MAPK: mitogen-activated protein kinases; PI3K: phosphoinositide 3-kinases; Akt: protein kinase B; STAT: signal transducer and activator of transcription.

Table 1. The top 10 most significantly enriched gene ontology (GO) classes for differentially expressed immune-related genes (DE-IRGs) (adjusted *p* value < 0.05).

IDs	Term	Adjusted *p*	Count
Biological process			
GO:0006959	Humoral immune response	2.64E−11	15
GO:0006956	Complement activation	1.85E−09	9
GO:0006935	Chemotaxis	2.95E−09	16
GO:0042330	Taxis	2.95E−09	16
GO:0042742	Defense response to bacterium	3.20E−09	14
GO:0019730	Antimicrobial humoral response	1.25E−08	10
GO:0002526	Acute inflammatory response	3.96E−08	9
GO:0002455	Humoral immune response mediated by circulating Immunoglobulin	2.26E−07	7
GO:0006958	Complement activation, classical pathway	1.66E−06	6
GO:0050853	B cell receptor signaling pathway	2.02E−06	7
Cellular component			
GO:0072562	Blood microparticle	5.68E−12	12
GO:0009897	External side of plasma membrane	1.73E−09	14
GO:0042571	Immunoglobulin complex, circulating	9.86E−09	5
GO:0062023	Collagen-containing extracellular matrix	4.11E−08	13
GO:0031093	Platelet alpha granule lumen	5.40E−08	7
GO:0031091	Platelet alpha granule	3.93E−07	7
GO:0071735	IgG immunoglobulin complex	1.20E−06	4
GO:0071745	IgA immunoglobulin complex	5.50E−05	3
GO:1905370	Serine-type endopeptidase complex	5.93E−05	3
GO:0034358	Plasma lipoprotein particle	5.93E−05	4
Molecular function			
GO:0034987	Immunoglobulin receptor binding	4.54E−07	5
GO:0005125	Cytokine activity	9.02E−07	10
GO:0005539	Glycosaminoglycan binding	9.02E−07	10
GO:0003823	Antigen binding	1.21E−05	8
GO:0019838	Growth factor binding	1.86E−05	7
GO:0005126	Cytokine receptor binding	1.86E−05	9
GO:0017046	Peptide hormone binding	2.58E−05	5
GO:0008083	Growth factor activity	4.73E−05	7
GO:0042277	Peptide binding	5.27E−05	9
GO:0008201	Heparin binding	6.09E−05	7

GO: Gene Ontology; IgG: immunoglobulin G; IgA: immunoglobulin A.

Table 2. The top 10 most meaningfully enriched pathways for differentially expressed immune-related genes (DE-IRGs) (adjusted *p* value < 0.05).

Pathway IDs	Pathway names	Adjusted *p*	Count
hsa04060	Cytokine-cytokine receptor interaction	1.83E−07	13
hsa04010	MAPK signaling pathway	3.15E−02	7
hsa04610	Complement and coagulation cascades	3.15E−02	4
hsa04145	Phagosome	3.15E−02	5
hsa04630	JAK-STAT signaling pathway	3.73E−02	5
hsa04151	PI3K-Akt signaling pathway	4.35E−02	7
hsa04917	Prolactin signaling pathway	9.71E−02	3
hsa01521	EGFR tyrosine kinase inhibitor resistance	1.19E−01	3
hsa04080	Neuroactive ligand-receptor interaction	1.25E−01	6
hsa04215	Apoptosis-multiple species	1.25E−01	2

MAPK: mitogen-activated protein kinase; JAK: Janus kinase; STAT: signal transducer and activator of transcription; PI3K: phosphoinositide 3-kinases; Akt: protein kinase B; EGFR: epidermal growth factor receptor.

Development of a prognostic prediction model according to risk score

To identify potential prognostic genes among the DE-IRGs, a univariate Cox regression analysis was conducted in the training cohort of HCC patients. Thirteen DE-IRGs were found to have significant associations with OS ($p < 0.01$) (Supplementary Table 3). Next, LASSO Cox regression analysis was performed to select genes and minimize the risk of overfitting. From the initial 13 DE-IRGs, eight were identified as the most informative genes for prognosis (Figure 6). These eight DE-IRGs were then utilized to build the prognostic predictive model through multivariate Cox regression analysis (Table 3). The risk score was calculated using the following formula:

Risk score = (BIRC5 expression × 0.09101) + (GHR expression × −0.05954) + (VIPR1 expression × −0.1469) + (ANGPTL1 expression × −0.11808) + (NR4A1 expression × −0.02885) + (IL33 expression × −0.07938) + (LECT2 expression × −0.08756) + (COLEC10 expression × −0.07007).

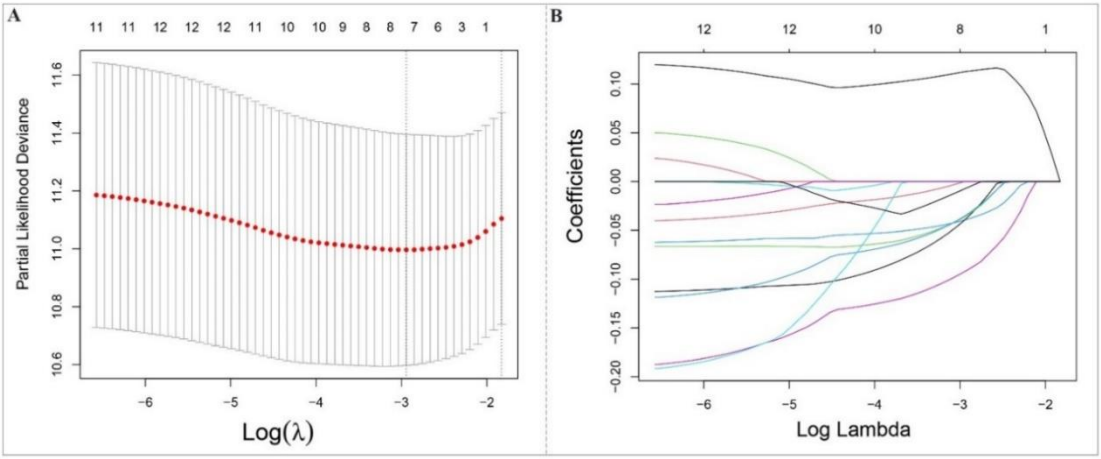

Figure 6. Building of prognostic prediction signature. A–B: Least absolute shrinkage and selection operator (LASSO) regression was employed to recognize the minimal criteria.

Table 3. Coefficients and multivariable Cox model results of the 8 immune-related genes in the risk signature.

	Gene	Coefficient	HR	HR (95% CI) Lower	HR (95% CI) Upper	*p*
1	*BIRC5*	0.09101	1.0953	0.9147	1.311	0.3220
2	*GHR*	−0.05954	0.9422	0.8214	1.081	0.3950
3	*VIPR1*	−0.14690	0.8634	0.6319	1.180	0.3564
4	*ANGPTL1*	−0.11808	0.8886	0.7544	1.047	0.1577
5	*NR4A1*	−0.02885	0.9716	0.8068	1.170	0.7608
6	*IL33*	−0.07938	0.9237	0.7596	1.123	0.4262
7	*LECT2*	−0.08756	0.9162	0.8341	1.006	0.0674
8	*COLEC10*	−0.07007	0.9323	0.7026	1.237	0.6273

HR: hazard ratio

The Prognostic Prediction Model Validation

The prognostic prediction model was validated based on the IRG signature using both the entire cohort and testing cohorts to evaluate its predictive capability. In all 3 cohorts, low- and high-risk groups were created for HCC patients using the optimal cutoff value of −0.5130. The model's ability to differentiate survival outcomes between these risk groups was then assessed. The results of KM curve analysis demonstrated a significant distinction in OS between the predicted low- and high-risk groups in all cohorts, indicating that patients classified as high-risk had a poorer prognosis (Figure 7A–C).

To evaluate the precision of the model, a time-dependent ROC curve analysis was executed. In the training cohort, the AUC values at one, three, and five years were 0.750, 0.733, and 0.699, respectively, representing the potential of the model to predict survival in HCC patients (Figure 7D). Also, the distribution of risk scores and survival conditions was examined within each cohort. The analysis revealed that patients with higher risk scores were more likely to experience poor survival outcomes (Figures 7G–L). Overall, these findings provide evidence of the immune-related gene signature's satisfactory predictive performance in the TCGA-LIHC dataset.

Assessing the Prognostic Prediction Model

The Model Showed a Correlation with the Clinicopathological Features

To gain further insights into the clinical relevance of the prognostic prediction model based on the 8-IRG risk score, we investigated the relationship between the risk score and various clinicopathological characteristics of patients with HCC. Through the Wilcoxon rank sum test, we found a significant correlation between the 8-IRG risk score and advanced clinical stage and T classification ($p < 0.01$) (Figure 8). This designates that patients with greater risk scores are more likely to have more advanced disease stages and larger tumor sizes. The observed association between the risk score and clinicopathological characteristics suggests that the prognostic significance of the model may be partially attributed to its correlation with these features.

The Model's Ability to Provide Prognostic Information Independently

To determine the autonomous or independent prognostic significance of the risk score according to the IRG signatures, univariable Cox regression analysis and multivariable Cox regression analysis were conducted. These analyses assessed the impact of various clinicopathological features on the predictive value of the risk score as an independent indicator. While factors such as advanced clinical stage, T and M stage, and high-risk score were associated with unfavorable OS outcomes, the most significant association was observed between OS and the risk score in the multivariable Cox regression analysis (HR=3.108, *p*=6.31e-06) (Figure 9). These data suggest the independent prognostic value of IRG signatures in HCC patients, irrespective of age, disease stage, and TNM classification.

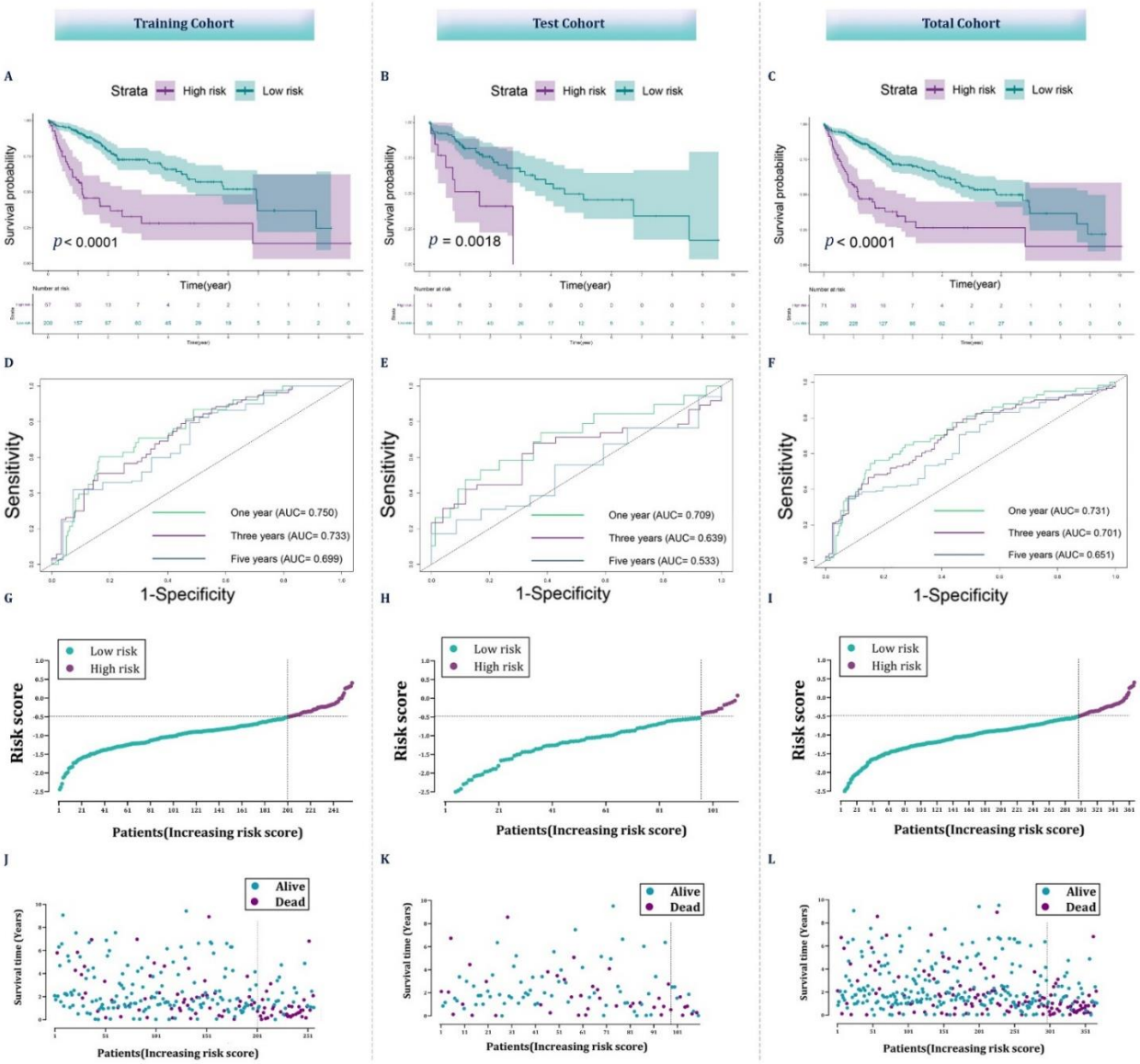

Figure 7. Confirmation of the immune-related signature in the cancer genome atlas (TCGA) cohort. A–C: Kaplan Meier curve analysis illustrating the survival differences between the high- and low-risk groups in all cohorts. D–F: Receiver operating characteristic (ROC) curve analysis of the model in all cohorts. G–L: Distribution of risk scores and survival status in all cohorts. AUC: area under the curve.

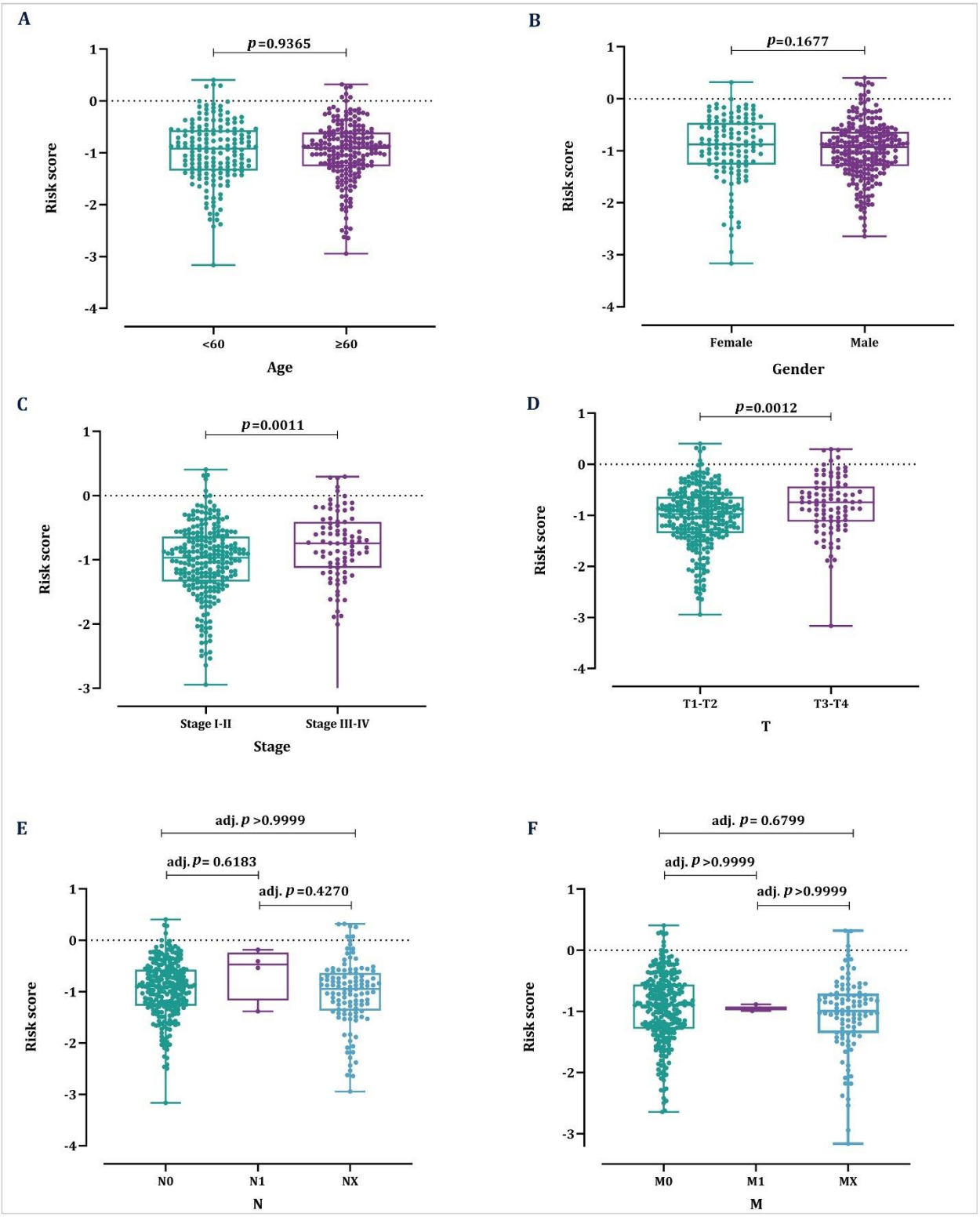

Figure 8. The relations between the immune-related risk signature and A: age; B: gender; C: clinical stage; D: T stage; E: N stage; F: M stage.

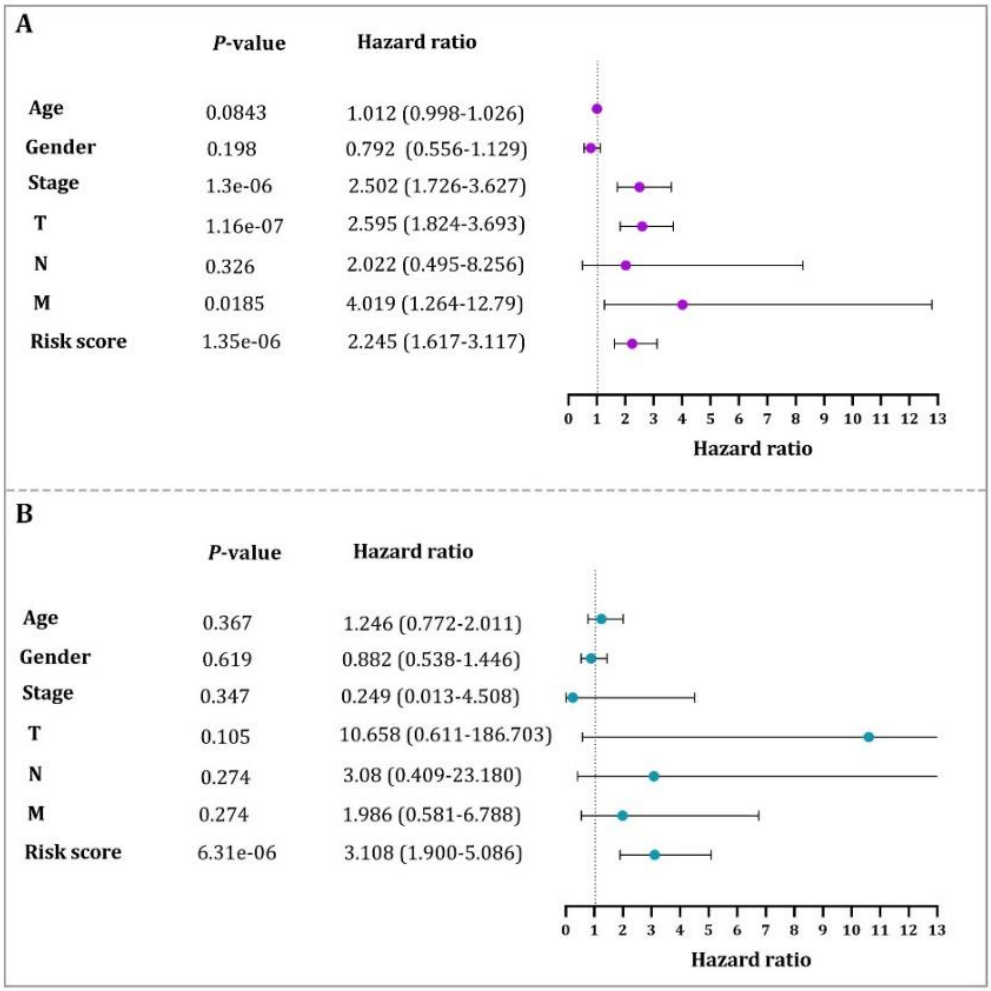

Figure 9. A: The findings of univariable Cox regression analysis in the entire cohort. B: The outcome of multivariable Cox regression analysis in the entire cohort.

The Risk Score Was Associated with Tumor-infiltrating Immune Cells

To better understand the tumor immune microenvironment in HCC patients, we examined the relationship between the risk score derived from the IRG signature and tumor-infiltrating immune cells (TIICs). The analysis revealed significant associations between the risk score and the proportions of various TIICs. In the high-risk group, there were significantly higher proportions of activated $CD4^+$ memory T cells (p=6.592e-08), $CD8^+$ T cells (p=0.001862), T follicular helper cells (p=0.00011), regulatory T cells (p =0.00265), resting natural killer cells (p=0.017), activated mast cells (p=0.002752), neutrophils (p=0.000629), macrophage M_0 (p=3.039e-05), and eosinophils (p=0.03834) (Figure 10A-10B). Spearman correlation analysis further confirmed positive correlations between the risk score and the proportions of activated $CD4^+$ memory T cells (p=6.10e-05), $CD8^+$ T cells (p=0.00018), T follicular helper cells (p=0.000176), regulatory T cells (p=2.62e-05), neutrophils (p=8.70e-05), macrophage M0 (p=4.85e-09), and plasma cells (p=0.003402) (Figure 10C). In contrast, some immune cells including resting $CD4^+$ memory T cells (p=1.29e-10), gamma delta T cells (p =0.03927), resting mast cells (p=0.002553), macrophage M1 (p=0.01941), macrophage M2 (p=0.0126), and monocytes (p=0.006347) showed negative associations with the risk scores in HCC patients (Figure 10C).

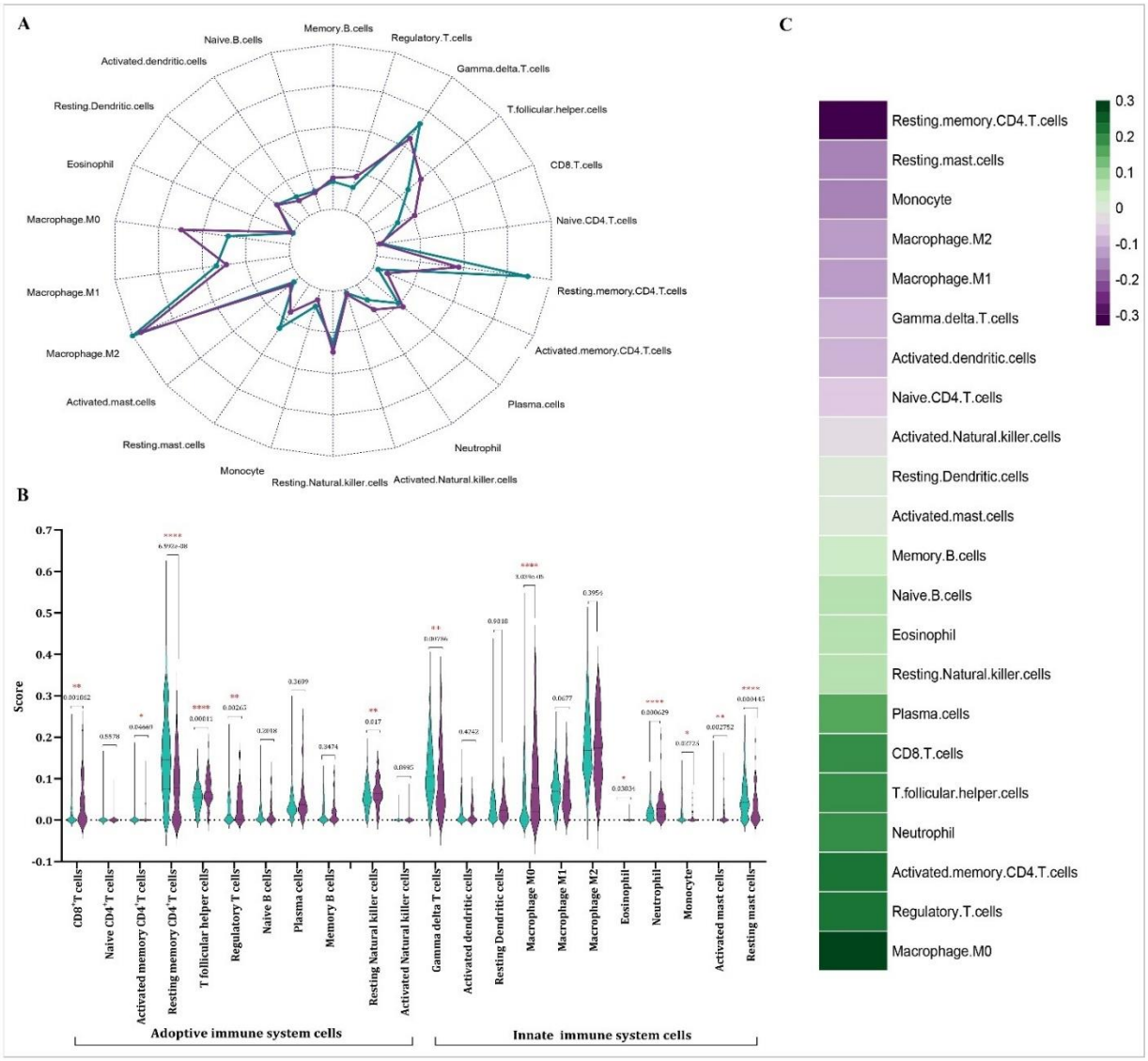

Figure 10. The correlation between risk score and Tumor-infiltrating Immune Cells (TIICs). A: The dissimilarity of TIICs between high- and low-risk groups. B: The violin plot depicts the dissimilarity of TIICs between high- and low-risk groups by *p*-value. The significance is depicted by asterisks. C) The Spearman correlation test among risk scores and TIICs.

Relation between the Risk Score and Mutation Profile

To explore the association between the risk score and the mutation profile in HCC patients, we analyzed the mutation status of each patient. Figures 11A and 11B illustrate the top 10 most significantly mutated genes in the low- and high-risk groups, respectively. Furthermore, we assessed the TMB for each sample and observed that the high-risk group had a significantly higher TMB compared to the low-risk group (p=0.0142) (Figure 11C). This proposes that high-risk patients tend to have a greater number of mutations in their tumor genomes compared to low-risk patients. Also, we performed a KM analysis to evaluate the link between TMB and OS. The results demonstrated a significant difference in OS between the high- and low-TMB groups, with high-TMB patients exhibiting worse outcomes (p=0.0081) (Figure 11D).

Nomogram Construction for Predicting Survival

To predict OS in HCC patients, we developed an OS predictive nomogram (Figure 12A). This graphical tool

combines multiple factors, including age, gender, TNM staging, stage, and the prognostic risk score model, to provide a comprehensive assessment of a patient's prognosis. The nomogram serves as a predictive model for estimating OS in HCC patients. To evaluate the precision and consistency of the nomogram, we assessed the calibration curves for the 3-year and 5-year time points (Figure 12B). The close alignment of predicted and observed outcomes in the calibration curves indicates the effectiveness of the nomogram in accurately predicting OS in HCC patients. In terms of prognostic performance, the nomogram had an AUC of 0.756 for the first year, demonstrating slightly superior prognostic ability compared to the prognostic risk score model, which had an AUC of 0.731 (Figure 12C).

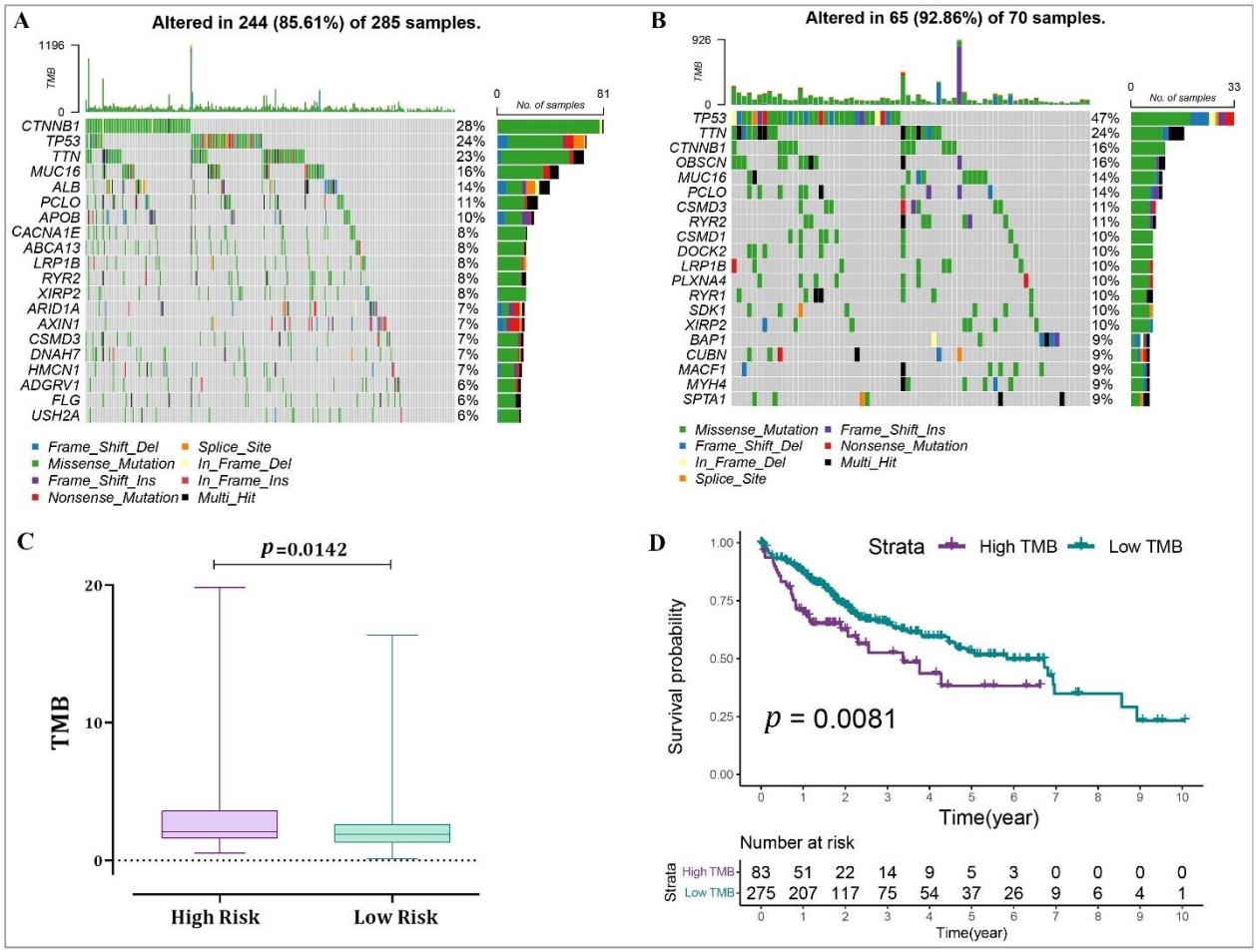

Figure 11. Tumor mutational burden (TMB) status between two risk groups. A: Low-risk group mutation profile. B: High-risk group mutation profile. C: A correlation analysis between TMB and risk score. D: The Kaplan Meier (KM) curve analysis of high- and low-TMB groups.

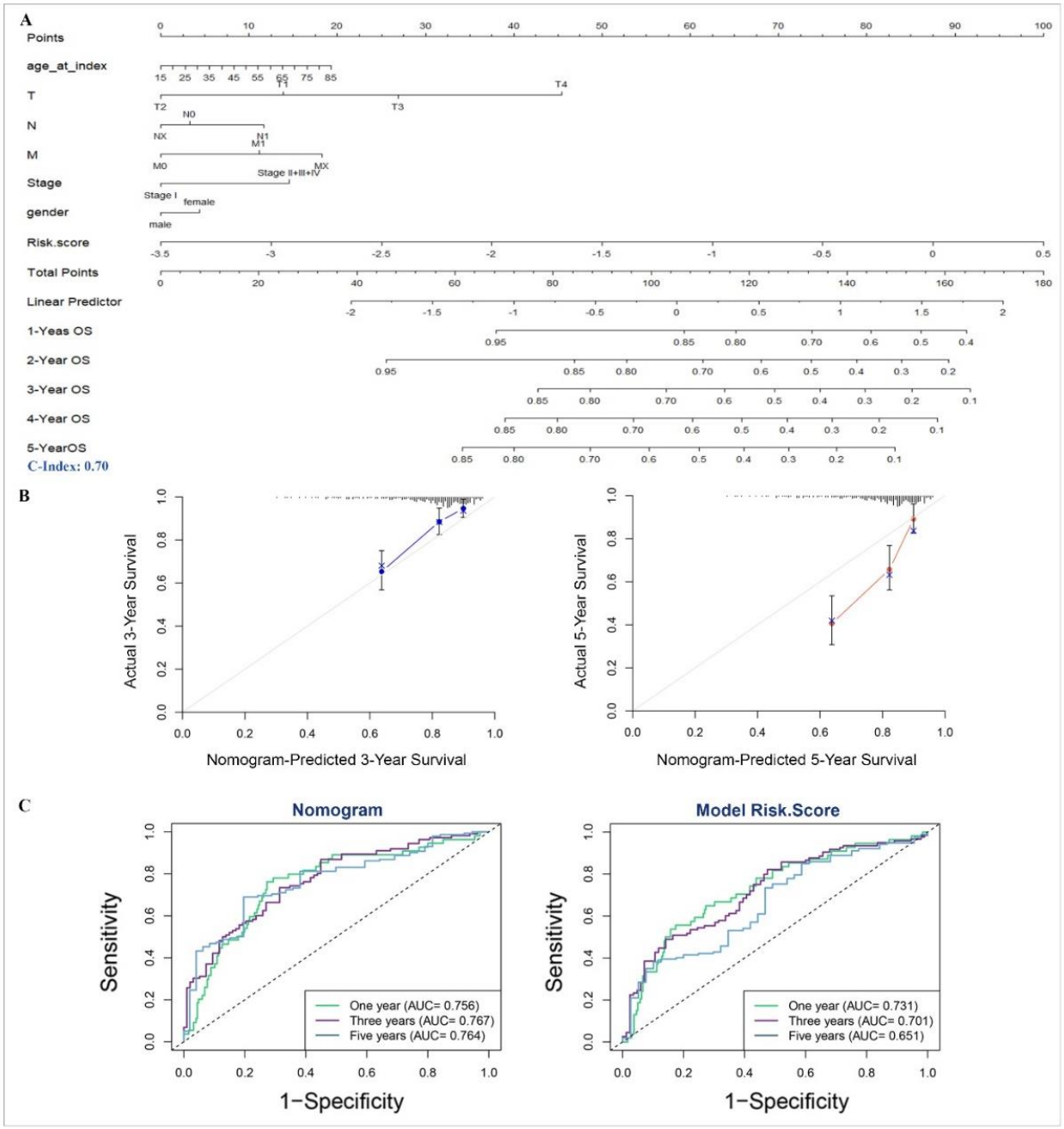

Figure 12. The predictive significance of the nomogram. A) The nomogram predicts the overall survival of hepatocellular carcinoma patients. B) Nomogram calibration plot. The x-axis shows the nomogram-predicted survival, and the observed survival is exhibited on the y-axis. C) Receiver operating characteristic (ROC) curves of the predictive efficiency of model risk score and nomogram.

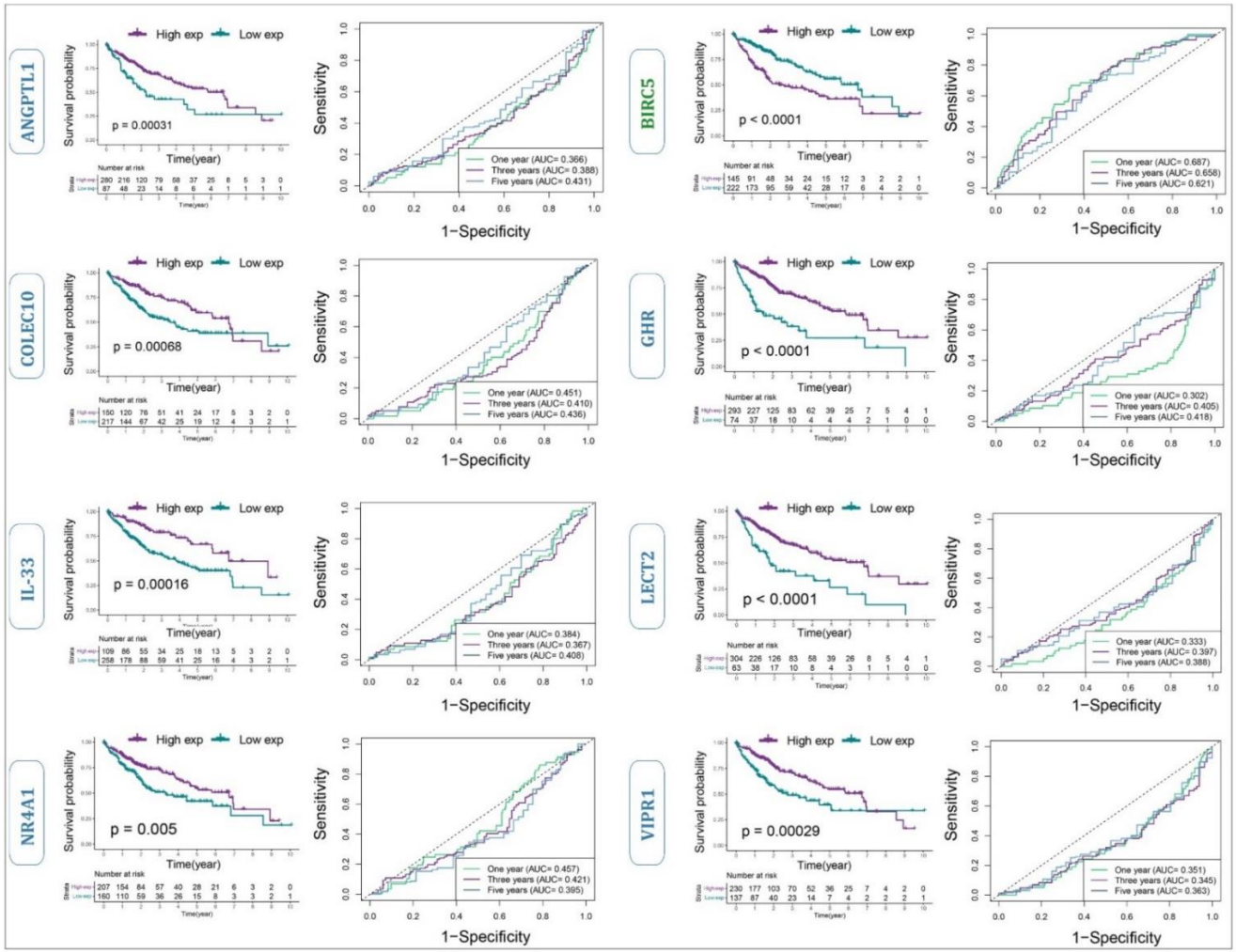

Figure 13. The Kaplan-Meier and Receiver Operating Characteristic (ROC) curves of 8 immune-related genes (IRGs) between high- and low-expression groups.

Building of lncRNA-miRNA-mRNA Regulatory Axis

Based on our results showing that BIRC5 is likely the main contributor in the 8-IRG prognostic model, we then constructed a lncRNA-miRNA-mRNA regulatory axis to further elucidate the potential molecular mechanism of this molecule. According to the results predicted by miRTargetLink and miRTarBase, 12 miRNAs were identified as potential targets of BIRC5 (Figure 14A). Among these miRNAs, hsa-miR-542, hsa-miR-218, hsa-miR-3613, and hsa-miR-335 were downregulated in HCC tissues compared to normal liver tissues (Figure 14B). The univariate Cox regression coefficient showed that among these 4 differently expressed miRNAs, only has-mir-542 has a prognostic value (*p* value=0.0107) (Figure 14C). To explore the upstream lncRNA targets of hsa-miR-542, we submitted it to LncBase and miRNet, which identified NEAT1 and C1orf220 as lncRNA targets (Figure 14E). Of note, we found that these two lncRNAs were upregulated in HCC tissues compared to normal liver tissues (Figure 14F).

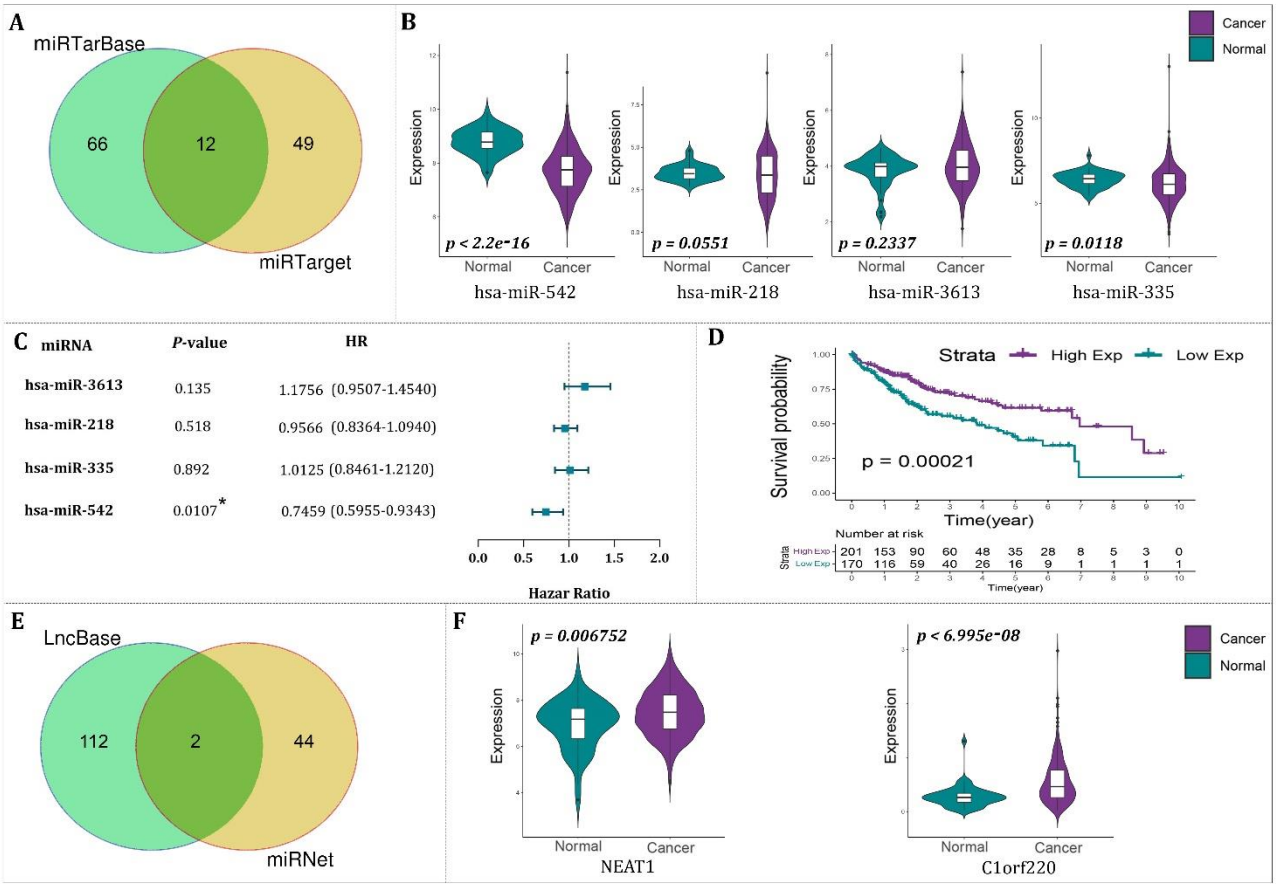

Figure 14. Building of lncRNA-miRNA-mRNA regulatory. A: The result of miRTarget and miRTarBase identified 12 miRNAs as potential miRNA targets of BIRC5. B: The expression of four miRNAs with a significant difference in their transcriptional activity in hepatocellular carcinoma tissues compared to normal liver tissues. C: The univariable COX regression analysis of four miRNAs. D: The relationship between has-miR-542 expression and overall survival of HCC patients. E: The result of LncBase and miRNet suggested NEAT1 and C1orf220 as lncRNA targets of has-miR-542. F) The expression of NEAT1 and C1orf22 in HCC tissues compared to normal liver tissues. Hsa: *Homo sapiens*; miR: microRNA; HR: hazard ratio; lncRNA: long noncoding RNA; mRNA: messenger RNA; BIRC5: survivin.

BIRC5 Inhibitor YM155 Reduced Metabolic Activity of HCC Cell Lines in a Concentration-manner

A number of preclinical surveys have stated that high expression of BIRC5 has been identified as a key molecule responsible for resistance to HCC treatments.[25,26] Given this and the findings obtained from our bioinformatics analyses, we aimed to evaluate the basal expression of BIRC5 in HCC cell lines. Intriguingly, our results revealed that HCC cell lines, including Huh7, HepG2, SNU449, and Hep3B2 expressed adequate levels of BIRC5 compared to GAPDH. Of note, while the Huh7 cell line displayed the lowest BIRC5 expression, HepG2 demonstrated a higher expression level of this gene compared to the other cell lines (Figure 15A). Next, we aimed to evaluate whether inhibiting this molecule could induce growth-suppressive effects. in the HepG2 cell line as these cells express significantly higher expression levels of BIRC5. As shown in Figure 15B, YM155 (a potent inhibitor of BIRC5) inhibited the metabolic activity of HepG2 in a concentration-dependent manner at 48 h; highlighting that BIRC5 may serve as a key contributor to survival in HepG2. To confirm the antiproliferative effects of the inhibitor in HCC cells, we also evaluated the drug's effect on Huh7, Hep3B2, and SNU449 as well. As expected, YM155 could significantly reduce the metabolic activity of all tested HCC cell lines. However, it is important to mention that there was no relation between the expression level of BIRC5 and response to the inhibitor, highlighting the complexity and multifactorial nature of the mechanisms involved in the response to the BIRC5 inhibitor (Figure 15C).

To explore the clinical utility of the risk score, the IC_{50} of YM155 was calculated, and drug sensitivity was compared between high- and low-risk HCC patients. As represented in Figure 15D, the IC_{50} of YM155 was significantly (p <0.0001) lower among the high-risk group, indicating this inhibitor would be more effective for patients in this group. This finding, coupled with the higher expression of BIRC5 in the high-risk group, suggests that the cells in the high-risk group are likely more dependent on the pro-survival functions of BIRC5 and, consequently, more vulnerable to therapeutic targeting of this protein by YM155.

DISCUSSION

During the preceding decades, the attention of many cancer researchers has turned toward the immune system as it has become increasingly clear that the intricate and dynamic relationship between the immune system and cancer cells can either promote tumor growth or mount a defense against them. One such area of interest is the role of the immune system in HCC, the most prevalent form of primary liver cancer. Recent studies have provided substantial evidence indicating that an imbalanced immune system can significantly contribute to HCC progression. This imbalance is characterized by changes in the quantity or function of immune cells, levels of cytokines, and the expression of inhibitory receptors or their ligands.[27,28] Indeed, alterations in the functionality or expression of immune elements redirect the immune response toward tumor tolerance, thereby promoting its progression. Overall, understanding the exact mechanisms through which the immune system interacts with hepatocellular tumor cells is crucial, as it can bring us a step closer to personalized medicine in HCC, at least partly, by enhancing patient stratification through the use of validated prognostic biomarkers.

In this study, we introduce a novel immune-related gene (IRG) signature that accurately predicts the survival of HCC patients. Notably, when combined with clinical data, this model displayed enhanced predictive capabilities. In this regard and to the best of our knowledge, no reports have yet described an immune-related gene signature consisting of BIRC5, GHR, VIPR1, ANGPTL1, NR4A1, LECT2, IL-33, and COLEC10 in HCC. Among these genes, only BIRC5 was up-regulated, while the others were down-regulated. We have compiled information about the constituents of this model and their roles in HCC and other cancer types, as shown in Table 4.

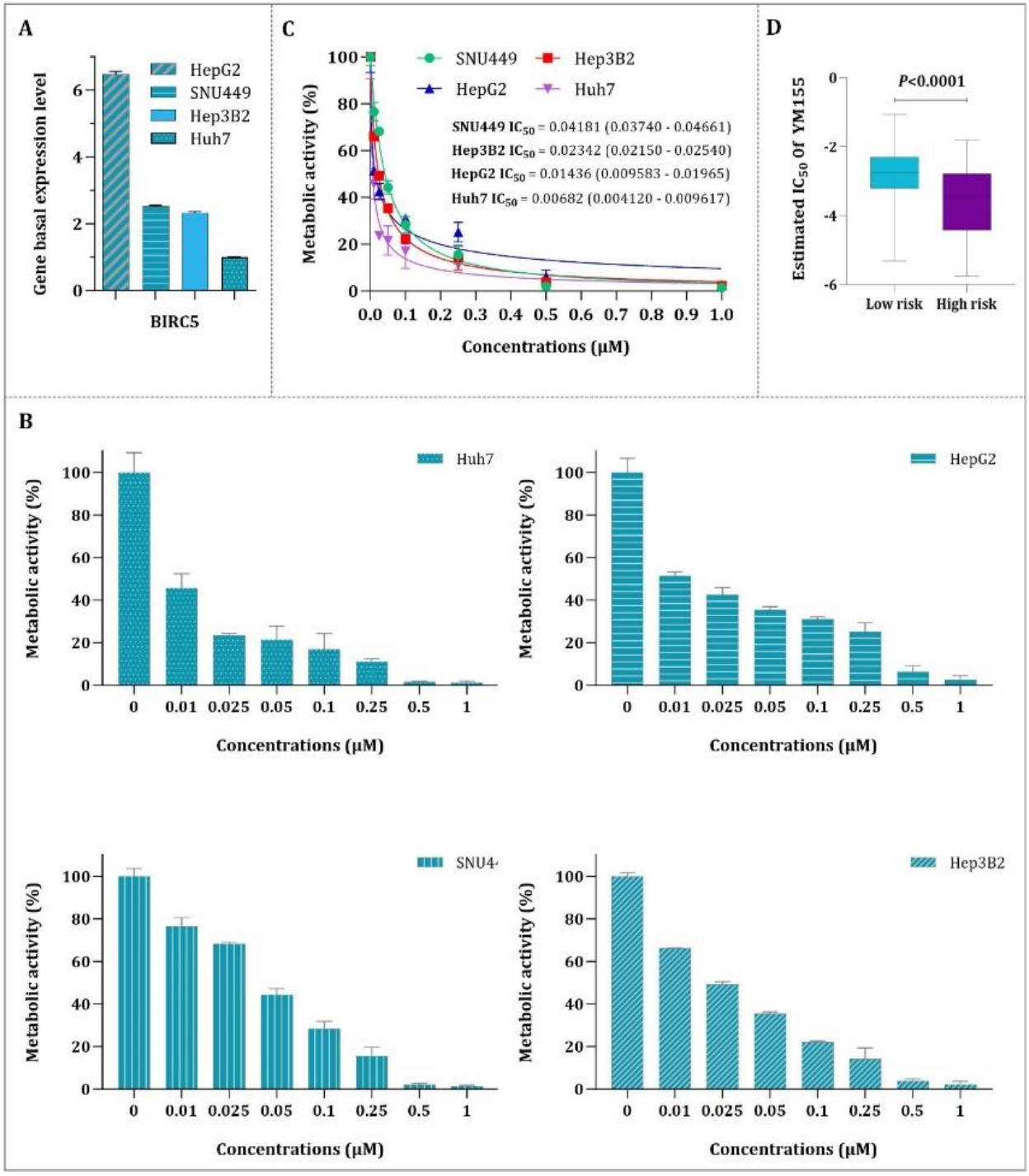

Figure 15. A: BIRC5 (Survivin) exhibits the highest expression in HepG2 compared to other cells. The basal expression of BIRC5 (normalized to GAPDH) is compared to its relative expression in Huh7, which has the lowest transcription of BIRC5 among the tested cell lines B: Sepantronium bromide (YM155) reduced the metabolic activity of all the tested HCC cell lines in a concentration-dependent manner. C: The highest and the lowest Half-maximal inhibitory concentration (IC_{50}) values were observed in the SNU449 and Huh7 cell lines, respectively. The values are presented as the mean ± standard deviation obtained from three independent experimental runs. D: The correlation between the sensitivity of YM155 (IC_{50}) and risk scores.

Table 4. The details of 8 differentially expressed immune-related genes (DE-IRGs) that are included in the model.

	Complete name	Function	Description
BIRC5	Baculoviral IAP repeat containing 5	Apoptosis Inhibition	The migration and invasion abilities of esophageal cancer cells are suppressed when BIRC5 is downregulated, as it interacts with the PI3K/Akt signaling pathway.[29] BIRC5 not only promotes the progression of laryngeal squamous cell carcinoma but also serves as a prognostic indicator for the disease.[30] In HCC, BIRC5 is overexpressed and plays crucial roles in promoting HCC cell survival and disease progression.[31] BIRC5 has been found to contribute to drug resistance in breast cancer cell lines.[32]
GHR	Growth hormone receptor	Cell Growth	Previous reviews have discussed the multiple mechanisms through which GH promotes cancer, including promoting cell proliferation, survival, epithelial to mesenchymal transition, migration, invasion, senescence, tumor growth, angiogenesis, metastasis, and resistance to drugs and radiation.[33-35] Breast cancer cells exhibit higher expression of GHR, and tumor expression of GH has been correlated with metastatic breast cancer and poor prognosis.[36]
VIPR1	Vasoactive Intestinal Peptide Receptor 1	Exocrine and endocrine secretion, and water and ion flux in lung and intestinal epithelia	By regulating arginine and pyrimidine metabolism, it acts as a suppressor of HCC progression.[37] VIPR1 shows promise as a potential biomarker for prostate cancer.[38]
ANGPTL1	Angiopoietin-related protein 1	Vascular endothelial growth factor	In colorectal cancer, ANGPTL1 attenuates cancer migration, invasion, and stemness by regulating the SOX2 expression via FOXO3a-mediated pathways.[39] ANGPTL1 has been shown to inhibit thyroid cancer cell proliferation, migration, and invasion. Additionally, its expression levels are lower in patients with recurrent differentiated thyroid cancer compared to those without recurrence.[40] ANGPTL1 expression positively correlates with sorafenib sensitivity in both HCC cells and human HCC tissues.[41]

Table 4. Continued...

	Complete name	Function	Description
NR4A1	Nuclear receptor subfamily 4 group A member 1	Cell cycle mediation, inflammation and apoptosis	The nuclear receptor NR4A1 acts as a tumor suppressor and is down-regulated in triple-negative breast cancer.[42] NR4A1-mediated apoptosis plays a role in suppressing lymphomagenesis and is associated with better cancer-specific survival in patients with aggressive B-cell lymphomas.[43] In HCC, NR4A1 mediates NK-cell dysfunction through the IFN-γ/p-STAT1/IRF1 pathway.[44] NR4A1 inhibits the epithelial-mesenchymal transition process in hepatic stellate cells.[45]
IL33	Interleukin 33	Innate and adaptive immune responses in mucosal organs	The killing function of $CD8^+$ T cells is enhanced by stimulation with recombinant IL-33.[46] Elevated levels of interleukin-33 in cancer cells and cancer-associated fibroblasts are associated with a favorable prognosis and suppressed migration in cholangiocarcinoma.[47] IL-33 has been shown to reduce tumor growth in models of colorectal cancer, with the assistance of eosinophils.[48]
LECT2	Leukocyte cell derived chemotaxin 2	Chemotactic factor for neutrophils	The expression of LECT2 is upregulated in normal tissue compared to liver tumor tissue.[49] LECT2 regulates the process of epithelial-mesenchymal transition and cancer stemness in HCC.[50]
COLEC10	Collectin subfamily member 10	Lectin complement pathway	Decreased expression of COLEC10 is a predictive factor for poor OS in patients with HCC.[51] By binding to GRP78, COLEC10 induces endoplasmic reticulum stress, thereby inhibiting progression of HCC.[52]

Akt: protein kinase B; BIRC5: survivin; CD8: cluster of differentiation 8; FOXO3: forkhead box protein O3; GH: growth hormone; GRP78: glucose-regulated protein 78; HCC: hepatocellular carcinoma; IFN: interferon; IL-33: interleukin-33; IRF: interferon-regulatory factor; OS: overall survival; PI3K: phosphoinositide 3-kinases; STAT: signal transducer and activator of transcription.

Our results indicated that this signature has a high level of accuracy in predicting the OS of HCC patients, as evidenced by the results of KM and ROC curve analyses. Importantly, the results of both univariate and multivariate Cox proportional regression analysis demonstrate that this signature independently serves as a prognostic factor. Notably, it can predict survival outcomes across various patient groups, including males and females, age groups <65 or >65 years old, different tumor stages (T1, T2, T3, or T4), lymph node involvement (N0 or N1 staging), and distant metastasis (M0 or M1 staging). In summary, even when considering these clinicopathological factors, the risk score derived from this signature remains a significant predictor of patient survival.

In a recent study, an IRG signature was established to predict the survival of patients with colorectal carcinoma (CRC). Based on the gene signature they designed scores in which patients with higher scores demonstrated a prolonged survival rate and vice versa. The gene signature was associated with age and clinical stage of the disease.", and high-score cases exhibited greater immune cell infiltration,[53] indicating that the developed gene signature could reflect the situation of tumors in CRC patients. In another study, a gene signature constructed from eight IRGs was able to predict OS and relapse-free survival (RFS)in patients with breast cancer. They stratified patients into high-risk and low-risk groups based on the gene signature and demonstrated that OS and RFS were shorter in high-risk cases compared with low-risk ones. The gene signature predicted the 3-year OS and 3-year RFS with AUC of 0.75 and 0.64, respectively. In the context of HCC, a gene signature composed of IRGs was shown to be associated with patient outcomes. This proposed gene signature correlated with the infiltration of macrophages and Tregs, however, no associations were evaluated regarding the situation of the tumor. They showed that the 3-year survival of HCC patients could be predicted using their gene signature, yielding an AUC of 0.71.[54] In contrast, our study demonstrated a higher AUC for a 3-year survival rate (AUC=0.73) and established an association between the gene signature and the tumor.

Recently, there has been growing evidence highlighting that the tumor microenvironment (TME) presents a certain challenge for effective therapies in HCC because it is intricately involved in metastasis and treatment resistance.[55] Our findings revealed that a higher risk score was associated with decreased infiltration of specific immune cell subsets crucial for immune surveillance and anti-tumor responses. These subsets include resting $CD4^+$ memory T cells, γδ-T cells, resting mast cells, and monocytes. The reasons for the low levels of resting memory T $CD4^+$ cells in the high-risk group of HCC patients are not yet fully understood; however, several factors may contribute to this phenomenon. Chronic inflammation, which is characteristic of HCC, can lead to the exhaustion or depletion of T cells, including resting memory T $CD4^+$ cells. In contrast to the high-risk group, spearman correlation analysis showed positive correlations between the risk score and the proportions of activated memory T $CD4^+$, T $CD8^+$, TFH cells, Treg cells, neutrophils, macrophage M0, and plasma cells. Figure 16 depicts the role of IRGs and TIM in the progression of HCC in the high-risk group through a schematic illustration.

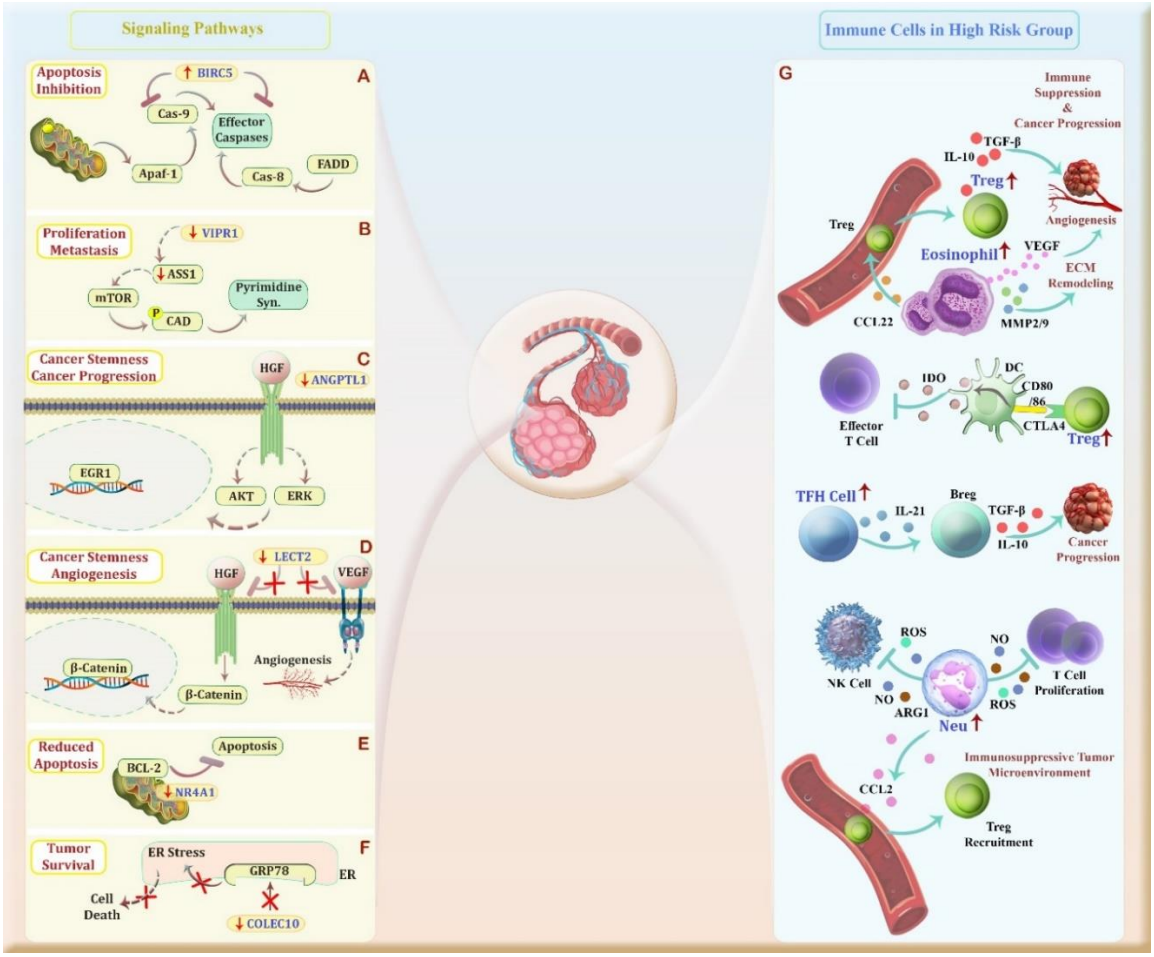

Figure 16. A schematic representation illustrating the role of Immune-related Genes (IRGs) and Tumor immune microenvironment (TIM) in the progression of hepatocellular carcinoma (HCC) in the high-risk group. A) Survivin, which is the product of the BIRC5 gene and functions as a suppressor of apoptosis, can suppress caspase activation by blocking pro-caspase-9 and obstructing its recruitment to Apaf-1. B) Down-regulation of VIPR1, which also leads to the down-regulation of ASS1, increases carbamoyl-phosphate synthetase 2, aspartate transcarbamylase, and dihydroorotase (CAD) phosphorylation in an mTOR/p70S6K signaling dependent manner, resulting in HCC proliferation and metastasis. C) When ANGPTL1 expression decreases, the hepatocyte growth factor gene (HGF) binds to its receptor and activates the AKT and ERK signaling pathway, leading to the progression of HCC. D) Decreased expression of the LECT2 gene removes its inhibitory effect on the HGF and VEGF receptors. This leads to the activation of the Wnt/β-Catenin signaling cascade and promotes angiogenesis. E) Apoptosis is inhibited through decreased expression of NR4A1 and increased activity of the anti-apoptotic gene BCL-2. F) Reduced ER stress due to decreased COLEC10 expression and its diminished binding to GRP78 leads to decreased cellular death and enhanced tumor survival. G) Increased eosinophil infiltration leads to Treg accumulation in the tumor microenvironment (TME), resulting in immune suppression. Additionally, eosinophils induce IDO production from dendritic cells (DCs), contributing to effector T-cell inhibition. MMP2/9 along with VEGF secreted from eosinophil, also promote extracellular matrix (ECM) remodeling and angiogenesis, respectively. In addition, the proliferation of B regulatory cells (Bregs) is induced by IL-21 secreted from T follicular helper (TFH) cells, resulting in immune suppression and tumor progression. The expansion of neutrophils, driven by increased Treg infiltration, along with the inhibition of NK cells and T cell proliferation by reactive oxygen species (ROS), nitric oxide (NO), and arginase 1 (ARG1),", creates an immunosuppressive TME leading to tumor progression.

STATEMENT OF ETHICS

This bioinformatics study analyzes data from The Cancer Genome Atlas (TCGA) and does not present any ethical issues, as the data is fully anonymized and does not contain identifiable patient information. (Ethics Code: IR.SBMU.RICH.REC.1402.007)

FUNDING

The study has not received any funding.

CONFLICT OF INTEREST

The authors declare no conflicts of interest.

ACKNOWLEDGEMENTS

The authors extend their appreciation to the Pediatric Infections Research Center, Research Institute for Children's Health, Shahid Beheshti University of Medical Sciences (Tehran, Iran) for their assistance and support in conducting this study. The findings presented in this paper are derived from the PhD thesis of Atieh Pourbagheri-Sigaroodi.

REFERENCES

1. Chidambaranathan-Reghupaty S, Fisher PB, Sarkar D. Hepatocellular carcinoma (HCC): Epidemiology, etiology and molecular classification. Advances in cancer research. 2021;149:1-61.
2. Samant H, Amiri HS, Zibari GB. Addressing the worldwide hepatocellular carcinoma: Epidemiology, prevention and management. Journal of gastrointestinal oncology. 2021;12(Suppl 2):S361.
3. Pinter M, Pinato DJ, Ramadori P, Heikenwalder M. NASH and Hepatocellular Carcinoma: Immunology and Immunotherapy. Clin Cancer Res. 2023;29(3):513-20.
4. Llovet JM, Kelley RK, Villanueva A, Singal AG, Pikarsky E, Roayaie S, et al. Hepatocellular carcinoma. Nat Rev Dis Primers. 2021;7(1):6.
5. Chen Z, Xie H, Hu M, Huang T, Hu Y, Sang N, Zhao Y. Recent progress in treatment of hepatocellular carcinoma. American journal of cancer research. 2020;10(9):2993.
6. Marin JJ, Macias RI, Monte MJ, Romero MR, Asensio M, Sanchez-Martin A, et al. Molecular bases of drug resistance in hepatocellular carcinoma. Cancers. 2020;12(6):1663.
7. Papaconstantinou D, Tsilimigras DI, Pawlik TM. Recurrent hepatocellular carcinoma: Patterns, detection, staging and treatment. Journal of Hepatocellular Carcinoma. 2022:947-57.
8. Hanahan D, Weinberg RA. Biological hallmarks of cancer. Holland-Frei Cancer Medicine. 2016:1-10.
9. Gnjatic S, Bronte V, Brunet LR, Butler MO, Disis ML, Galon J, et al. Identifying baseline immune-related biomarkers to predict clinical outcome of immunotherapy. Journal for immunotherapy of cancer. 2017;5(1):1-18.
10. Ge P, Wang W, Li L, Zhang G, Gao Z, Tang Z, et al. Profiles of immune cell infiltration and immune-related genes in the tumor microenvironment of colorectal cancer. Biomedicine & Pharmacotherapy. 2019;118:109228.
11. Chen P, Yang Y, Zhang Y, Jiang S, Li X, Wan J. Identification of prognostic immune-related genes in the tumor microenvironment of endometrial cancer. Aging (Albany NY). 2020;12(4):3371.
12. Jiang B, Sun Q, Tong Y, Wang Y, Ma H, Xia X, et al. An immune-related gene signature predicts prognosis of gastric cancer. Medicine. 2019;98(27).
13. Bou-Dargham MJ, Sha L, Sang Q-XA, Zhang J. Immune landscape of human prostate cancer: immune evasion mechanisms and biomarkers for personalized immunotherapy. BMC cancer. 2020;20:1-10.
14. Fu M, Wang Q, Wang H, Dai Y, Wang J, Kang W, et al. Immune-related genes are prognostic markers for prostate cancer recurrence. Frontiers in Genetics. 2021;12:639642.
15. Liao R, Ma Q-Z, Zhou C-Y, Li J-J, Weng N-N, Yang Y, Zhu Q. Identification of biomarkers related to Tumor-Infiltrating Lymphocytes (TILs) infiltration with gene co-expression network in colorectal cancer. Bioengineered. 2021;12(1):1676-88.
16. Kim S, Kim JR, Lee JH, Moon S-H, In Jo S, Bae D-J, et al. Differential RNA expression of immune-related genes and tumor cell proximity from intratumoral M1 macrophages in acral lentiginous melanomas treated with PD-1 blockade. Biochimica et Biophysica Acta (BBA) - Molecular Basis of Disease. 2022;1868(11):166516.
17. Huang M, Liu L, Zhu J, Jin T, Chen Y, Xu L, et al. Identification of immune-related subtypes and characterization of tumor microenvironment infiltration in bladder cancer. Frontiers in Cell and Developmental Biology. 2021;9:723817.
18. Ritchie ME, Phipson B, Wu D, Hu Y, Law CW, Shi W, Smyth GK. limma powers differential expression analyses for RNA-sequencing and microarray studies. Nucleic acids research. 2015;43(7):e47-e.

19. Yu G, Wang L-G, Han Y, He Q-Y. clusterProfiler: an R package for comparing biological themes among gene clusters. Omics: a journal of integrative biology. 2012;16(5):284-7.
20. Wang H, Lengerich BJ, Aragam B, Xing EP. Precision Lasso: accounting for correlations and linear dependencies in high-dimensional genomic data. Bioinformatics. 2019;35(7):1181-7.
21. Heagerty PJ, Saha-Chaudhuri P, Saha-Chaudhuri MP. Package 'survivalROC'. San Francisco: GitHub. 2013.
22. Mayakonda A, Lin D-C, Assenov Y, Plass C, Koeffler HP. Maftools: efficient and comprehensive analysis of somatic variants in cancer. Genome research. 2018;28(11):1747-56.
23. Kolde R, Kolde MR. Package 'pheatmap'. R package. 2015;1(7):790.
24. Villanueva RAM, Chen ZJ. ggplot2: elegant graphics for data analysis. Taylor & Francis; 2019.
25. Sun T, Mao W, Peng H, Wang Q, Jiao L. YAP promotes sorafenib resistance in hepatocellular carcinoma by upregulating survivin. Cell Oncol (Dordr). 2021;44(3):689-99.
26. Namgung Y, Kim SY, Kim I. Down-regulation of Survivin by BIX-01294 pretreatment overcomes resistance of hepatocellular carcinoma cells to TRAIL. Anticancer Research. 2019;39(7):3571-8.
27. Aravalli RN. Role of innate immunity in the development of hepatocellular carcinoma. World journal of gastroenterology: WJG. 2013;19(43):7500.
28. Llovet JM, Castet F, Heikenwalder M, Maini MK, Mazzaferro V, Pinato DJ, et al. Immunotherapies for hepatocellular carcinoma. Nature reviews Clinical oncology. 2022;19(3):151-72.
29. Shang X, Liu G, Zhang Y, Tang P, Zhang H, Jiang H, Yu Z. Downregulation of BIRC5 inhibits the migration and invasion of esophageal cancer cells by interacting with the PI3K/Akt signaling pathway. Oncology letters. 2018;16(3):3373-9.
30. Wang N, Huang X, Cheng J. BIRC5 promotes cancer progression and predicts prognosis in laryngeal squamous cell carcinoma. PeerJ. 2022;10:e12871.
31. Li Y, Zhao Z-G, Luo Y, Cui H, Wang H-Y, Jia Y-F, Gao Y-T. Dual targeting of Polo-like kinase 1 and baculoviral inhibitor of apoptosis repeat-containing 5 in TP53-mutated hepatocellular carcinoma. World Journal of Gastroenterology. 2020;26(32):4786.
32. de Moraes GN, Delbue D, Silva KL, Robaina MC, Khongkow P, Gomes AR, et al. FOXM1 targets XIAP and Survivin to modulate breast cancer survival and chemoresistance. Cellular signalling. 2015;27(12):2496-505.
33. Brittain AL, Basu R, Qian Y, Kopchick JJ. Growth hormone and the epithelial-to-mesenchymal transition. The Journal of Clinical Endocrinology & Metabolism. 2017;102(10):3662-73.
34. Basu R, Kopchick JJ. The effects of growth hormone on therapy resistance in cancer. Cancer Drug Resistance. 2019;2(3):827.
35. Kopchick JJ, Basu R, Berryman DE, Jorgensen JO, Johannsson G, Puri V. Covert actions of growth hormone: fibrosis, cardiovascular diseases and cancer. Nature Reviews Endocrinology. 2022;18(9):558-73.
36. Gebre-Medhin M, Kindblom L-G, Wennbo H, Törnell J, Meis-Kindblom JM. Growth hormone receptor is expressed in human breast cancer. The American journal of pathology. 2001;158(4):1217-22.
37. Fu Y, Liu S, Rodrigues RM, Han Y, Guo C, Zhu Z, et al. Activation of VIPR1 suppresses hepatocellular carcinoma progression by regulating arginine and pyrimidine metabolism. Int J Biol Sci. 2022;18(11):4341-56.
38. Aliyu M, Saboor-Yaraghi AA, Nejati S, Robat-Jazi B. Urinary VPAC1: A potential biomarker in prostate cancer. AIMS Allergy and Immunology. 2022;6(2):42-63.
39. Chang T-Y, Lan K-C, Chiu C-Y, Sheu M-L, Liu S-H. ANGPTL1 attenuates cancer migration, invasion, and stemness through regulating FOXO3a-mediated SOX2 expression in colorectal cancer. Clinical Science. 2022;136(9):657-73.
40. Sun R, Yang L, Hu Y, Wang Y, Zhang Q, Zhang Y, et al. ANGPTL1 is a potential biomarker for differentiated thyroid cancer diagnosis and recurrence. Oncology Letters. 2020;20(5):1-.
41. Chen HA, Kuo TC, Tseng CF, Ma JT, Yang ST, Yen CJ, et al. Angiopoietin-like protein 1 antagonizes MET receptor activity to repress sorafenib resistance and cancer stemness in hepatocellular carcinoma. Hepatology. 2016;64(5):1637-51.
42. Wu H, Bi J, Peng Y, Huo L, Yu X, Yang Z, et al. Nuclear receptor NR4A1 is a tumor suppressor down-regulated in triple-negative breast cancer. Oncotarget. 2017;8(33):54364.
43. Deutsch AJ, Rinner B, Wenzl K, Pichler M, Troppan K, Steinbauer E, et al. NR4A1-mediated apoptosis suppresses lymphomagenesis and is associated with a favorable cancer-specific survival in patients with aggressive B-cell lymphomas. Blood, The Journal of the American Society of Hematology. 2014;123(15):2367-77.

44. Yu W, He J, Wang F, He Q, Shi Y, Tao X, Sun B. NR4A1 mediates NK-cell dysfunction in hepatocellular carcinoma via the IFN-γ/p-STAT1/IRF1 pathway. Immunology. 2023;169(1):69-82.
45. Huang Q, Xu J, Ge Y, Shi Y, Wang F, Zhu M. NR4A1 inhibits the epithelial–mesenchymal transition of hepatic stellate cells: Involvement of TGF-β–Smad2/3/4–ZEB signaling. Open Life Sciences. 2022;17(1):447-54.
46. WANG H, LIU Y, LI D, SHEN G. Expression of interleukin-33 in hepatocellular carcinoma patients and its role in regulating CD8. Journal of Clinical Hepatology. 2022:117-23.
47. Yangngam S, Thongchot S, Pongpaibul A, Vaeteewoottacharn K, Pinlaor S, Thuwajit P, et al. High level of interleukin-33 in cancer cells and cancer-associated fibroblasts correlates with good prognosis and suppressed migration in cholangiocarcinoma. Journal of Cancer. 2020;11(22):6571.
48. Kienzl M, Hasenoehrl C, Valadez-Cosmes P, Maitz K, Sarsembayeva A, Sturm E, et al. IL-33 reduces tumor growth in models of colorectal cancer with the help of eosinophils. Oncoimmunology. 2020;9(1):1776059.
49. Zhou Y, Ran X, Han M. Identification of a immune-related gene signature as a novel prognostic biomarker of cholangiocarcinoma. 2023.
50. Chu T-H, Ko C-Y, Tai P-H, Chang Y-C, Huang C-C, Wu T-Y, et al. Leukocyte cell-derived chemotaxin 2 regulates epithelial-mesenchymal transition and cancer stemness in hepatocellular carcinoma. Journal of Biological Chemistry. 2022;298(10).
51. Zhang B, Wu H. Decreased expression of COLEC10 predicts poor overall survival in patients with hepatocellular carcinoma. Cancer management and research. 2018:2369-75.
52. Cai M-N, Chen D-M, Xiao L-X, Li S-S, Liao C-H, Li J, et al. COLEC10 Induces Endoplasmic Reticulum Stress by Occupying GRP78 and Inhibits Hepatocellular Carcinoma. Laboratory Investigation. 2023;103(7):100130.
53. Kang Z, Chen B, Ma X, Yan F, Wang Z. Immune-related gene-based model predicts the survival of colorectal carcinoma and reflected various biological statuses. Front Mol Biosci. 2023;10:1277933.
54. Chen R, Zhao M, An Y, Liu D, Tang Q, Teng G. A Prognostic Gene Signature for Hepatocellular Carcinoma. Front Oncol. 2022;12:841530.
55. Zhang J, Han H, Wang L, Wang W, Yang M, Qin Y. Overcoming the therapeutic resistance of hepatomas by targeting the tumor microenvironment. Front Oncol. 2022;12:988956.